

Review

Open Access



# Process parameter optimization of metal additive manufacturing: a review and outlook

Hou Yi Chia, Jianzhao Wu, Xinzhi Wang, Wentao Yan\*

Department of Mechanical Engineering, National University of Singapore, Singapore 117575, Singapore.

\*Correspondence to: Assistant Prof. Wentao Yan, Department of Mechanical Engineering, National University of Singapore, Singapore 117575, Singapore. E-mail: mpeyanw@nus.edu.sg ; ORCID: 0000-0001-8480-6375

How to cite this article: Chia HY, Wu J, Wang X, Yan W. Process parameter optimization of metal additive manufacturing: a review and outlook. *J Mater Inf* 2022;2:16. <http://dx.doi.org/10.20517/jmi.2022.18>

Received: 30 Jun 2022 First Decision: 4 Aug 2022 Revised: 1 Sep 2022 Accepted: 13 Sep 2022 Published: 9 Oct 2022

Academic Editors: Xingjun Liu, Qian Li Copy Editor: Jia-Xin Zhang Production Editor: Jia-Xin Zhang

## Abstract

The selection of appropriate process parameters is crucial in metal additive manufacturing (AM) as it directly influences the defect formation and microstructure of the printed part. Over the past decade, research efforts have been devoted to identifying “optimal” processing regimes for different materials to achieve defect-free manufacturing, which mostly involve costly trial-and-error experiments and computationally expensive mechanistic simulations. Hence, it is apropos to critically review the methods used to achieve the optimal process parameters in AM. This work seeks to provide a structured analysis of current methodologies and discuss systematic approaches toward general optimization work in AM and the process parameter optimization of new AM alloys. A brief review of process-induced defects due to process parameter selection is given and the current methods for identifying “optimal processing windows” are summarized. Research works are analyzed under a standard optimization framework, including the design of experiments and characterization, modelling and optimization algorithms. The research gaps that preclude multi-objective optimization in AM are identified and future directions toward optimization work in AM are discussed. With growing capabilities in AM, we should reconsider the definition of the “optimal processing region”.

**Keywords:** Additive manufacturing, process parameters, optimization, modeling, design of experiments

## INTRODUCTION

Metal-based additive manufacturing (AM) has many methodological variants, including powder bed fusion (PBF), electron beam melting (EBM), direct energy deposition (DED), wire-arc additive manufacturing (WAAM) and binder jetting (BJ). Regardless of the method used, metal AM processes involve a plethora of process pa-



© The Author(s) 2022. **Open Access** This article is licensed under a Creative Commons Attribution 4.0 International License (<https://creativecommons.org/licenses/by/4.0/>), which permits unrestricted use, sharing, adaptation, distribution and reproduction in any medium or format, for any purpose, even commercially, as long as you give appropriate credit to the original author(s) and the source, provide a link to the Creative Commons license, and indicate if changes were made.



parameters that influence the usually high heat input and cooling rates (except in processes without localized heat sources, e.g., BJ). The thermal history of the AM process affects the microstructure of the AM part, which consequently affects its mechanical properties, such as tensile strength, ductility, surface roughness, fatigue life and hardness. Hence, a proper understanding and optimal control of the process parameters are key to producing quality AM parts. Therefore, for any given design objective, manufacturing objective and feedstock material, optimal process parameters should be determined.

Nevertheless, the optimization of process parameters in AM is a challenging endeavor, owing to the wide process space and parameter selection. More importantly, minute variations in processing parameters affect the cooling rate and heat input, therefore requiring more careful control during processing for consistency and reliability. It is clear that the large parameter space in AM requires more sophisticated approaches for optimization rather than simple trial and error.

Without standardized parameter selection criteria, certification remains a major roadblock for metal AM to be widely applied in industry<sup>[1]</sup>. A key reason is the lack of suitable metrics for quality and control, of which process parameters are the inherent prerequisites. According to the AMSC Roadmap published in 2018<sup>[2]</sup>, parameter control has been identified as a research gap (PC5 and QC3) due to the many sources of variability during the AM process. As a complete understanding is currently unavailable, qualification can only be obtained through qualification test pieces of various geometries. In its subsequent update in 2022<sup>[3]</sup>, standards have been developed to address the issue, but these published standards contain no quantitative description or requirements for process parameter selection. Moreover, ISO/ASTM 52910:2018(E) standard<sup>[4]</sup> has identified that considerable time can be spent on experimental iteration to determine the optimal process parameters, thereby increasing the upfront engineering costs. Hence, the trial-and-error method of determining the optimized process parameters can easily deter interested parties from utilizing AM due to its cost-ineffectiveness. Most companies also treat process parameter control as intellectual property to retain a competitive advantage. Therefore, a universal indicator for part quality is highly coveted. The AMSC suggested a single (or few) process parameter(s) that can combine both material and process parameters independent of the material and machine. For example, the NASA MFSC SPEC 3717 standard suggests the use of top melt pool characterization and melt pool depth and width measurements as informative of process health. Therefore, process parameter optimization is directly connected to the issue of standardization and is a highly relevant problem for industry.

In AM, the optimization of process parameters first begins by identifying a suitable processing map for a given material. Over the past decade, efforts have been focused on processing regions with near-zero defects. Thereafter, a suitable combination of parameters within this processing window is then identified according to the design objectives of the AM user. As the change in process parameters usually leads to conflicting objectives, the optimization of process parameters in AM is effectively a multi-objective optimization engineering problem. Ideally, the optimization procedure should consider multiscale and transient effects unique to the AM process.

To perform an effective optimization, accurate and reliable models that relate the process parameters to their properties are required. The understanding of these process-structure-property (PSP) relations is therefore crucial and is determined through combined efforts in experiments and simulations. If a sufficiently rigorous PSP model is defined, different algorithms can be applied with the PSP model as a fitness function to perform a multi-objective optimization study. However, it is often the case that a complete description of the complex physical mechanisms occurring in metal AM is not immediately available or remains lacking. Although powerful and accurate mechanistic numerical models have been developed, they remain computationally expensive. Consequently, experimental optimization methods are usually still performed and surrogate models are developed, from basic methods, such as surface regression, to more sophisticated methods, such as machine learning (ML). Due to the complexity of the physical process, ML has recently gained traction in AM research

as a useful tool to identify PSP relations and provide sufficiently accurate predictions for optimization.

There is abundant literature on the process parameter optimization of different metal AM materials and numerous review articles on the topic of AM. These articles acknowledge and highlight the need for process parameter optimization in AM. However, there has been no attempt to summarize and evaluate the methods used to achieve optimal process parameters in AM. The objective of this work is to critically review the methods of optimization of process parameters in AM research and outline possible research directions and optimization strategies. We believe such a review will be especially helpful in the process optimization of new AM alloys and general optimization work for AM practitioners. In this review, literature on the optimization of process parameters in AM is compiled and systematically classified under the traditional optimizing framework of design of experiments (DoE) and modelling and optimization. A brief review on the defects due to inappropriate defect selection and optimal processing window is given to provide context for discussion. The effectiveness, limitations and potential of the optimization work carried out in AM are discussed and possible research gaps are suggested.

## PROCESS PARAMETERS AND DEFECT FORMATION IN METAL AM

The main goal of manufacturing is to create a functional part. Ideally, a functional part of superior quality requires the manufactured part to be defect-free. This is especially true in metal processing for most engineering applications, where micro-defects, such as pores, generally act as crack and fatigue initiation sites, resulting in deterioration of the mechanical properties. Technologies in metal AM are largely derived from powder metallurgy, wherein the relative density of the green part is crucial to its mechanical properties. Consequently, the notion of “process parameter optimization” in the past decade has been used to identify the process space for minimum porosity<sup>[5–7]</sup>.

In metal AM methods that utilize local concentrated heat sources (e.g., PBF, EBM, DED and WAAM), the defects are grouped into two main categories based on their severity, which have been identified and studied<sup>[7–10]</sup>, namely, (i) pores and voids and (ii) cracks, delaminations or distortions. Pores and voids are the main defect in AM parts with no significant distortion, delamination or cracking. In contrast, cracks, delaminations and distortions (which can arise due to pores) are more severe as they render the manufactured part unusable, disrupt the manufacturing process, and have the potential to cause direct harm to the machine itself, e.g., distorted or delaminated parts may collide with the recoater blade or drum in PBF processes, or the deposition nozzle in DED processes. Most machines with a fail-safe mechanism will directly halt the manufacturing process if any collision events are detected. For minor distortions and cracks, the manufacturing process may not be disrupted as there will be no significant detectable collisions. However, the part will become unusable and can only be inspected after retrieval from the manufacturing chamber. Similarly, if significant distortion occurs, the machine may halt and the part formed from the previous layers would be unusable. In both cases, it is a waste of time, effort and material. Regardless of the manufacturing method, all the aforementioned defects arise due to an inappropriate combination of process parameters and any defects should be mitigated or even exploited to achieve a superior part.

Pores and voids can be largely classified into a lack of fusion defects, gas porosities and keyhole porosities, all of which occur under different process parameter combinations. Currently, relative densities greater than 99% are easily achievable<sup>[11–13]</sup>. However, the existence of porosities should not be of primary concern; rather, the formation mechanisms and morphology of these pores play a greater role in determining the mechanical properties. Gong *et al.* showed that parts with keyhole porosities of 1% had little effect on tensile strength, while a lack of fusion porosities of the same level had a detrimental effect on the mechanical properties<sup>[14]</sup>. In fact, under static loading conditions, small porosities lower than a critical size (dependent on material) may be harmless<sup>[15]</sup>. The morphology of such pores are more significant, where Kasperovich *et al.* suggested that

sharp irregularities in the pores can act as stress concentrators based on classification of the voids via principal curvature analysis<sup>[16]</sup>. Moreover, Snow *et al.* highlighted that the formation of such pores and voids may be partly stochastic, as the complete systematic control of certain conditions, such as power fluctuations, particle packing and spatter, remains intractable<sup>[17]</sup>. Hence, it is clear that it is not the existence of pores that determines the part quality, but instead its geometry and formation mechanism. Given the prevalence and susceptibility of the formation of pores, the complete elimination of pores and voids is impractical and unnecessary. Therefore, admissible pores should be considered depending on the application of the AM part.

More importantly, processing parameters have a direct influence on type-I macro-residual stresses in AM, induced by the rapid cyclical heating and cooling during processing<sup>[18,19]</sup>. These high residual stresses may induce cracks<sup>[20–23]</sup>, delaminations<sup>[24]</sup> and distortions<sup>[25,26]</sup>. Bartlett *et al.* concluded from several studies that the lowest possible (effective) energy input should be used to minimize residual stresses<sup>[27]</sup>. While the mitigation of residual stresses via control of process parameters is a solution, base plate preheating can partly reduce the magnitude of residual stresses and mitigate the problems induced by residual stresses<sup>[28–33]</sup>. However, this solution comes at the expense of reduced mechanical performance, as larger grain sizes are obtained due to lower cooling rates. Moreover, the preheating temperature has to be designed according to the thermodynamic system of the alloy. If the preheating temperature exceeds a threshold, undesirable microstructures may adversely affect the mechanical properties of the material<sup>[32]</sup>. Furthermore, preheating requires higher energy consumption during processing and the careful design of thermal control of the base plate to ensure even and homogeneous heating. Hence, it is still desirable to directly control the residual stress characteristics via process parameter selection.

In addition to the aforementioned defects, physical phenomena arising from parameter selection can be further exploited to enhance the quality of AM parts. Notably, the parameters of the processing atmosphere have been shown to have a significant influence on the AM part. The pressure of the chamber may be adjusted to control the melt pool morphology<sup>[34]</sup> and keyhole stability<sup>[35]</sup>. Under specific processing conditions, the in-situ nano-oxides that form may induce inoculation and beneficial grain refinement effects<sup>[36,37]</sup>. Moreover, Ikehata *et al.* demonstrated that the use of different gas atmospheres and their concentration can be calibrated to achieve grain refinement, suggesting that even the gas content in the chamber is a potential processing parameter<sup>[38]</sup>. The nominal laser power delivered to the powder bed can also be reduced by the shielding gas properties<sup>[39]</sup>. Moreover, the control of the shielding gas type and velocities affect the printed quality. The shielding gas velocities can disrupt the powder bed and affect the porosity<sup>[39,40]</sup>. In addition, the shielding gas can directly influence the vapor plume characteristics<sup>[39,41,42]</sup>, where the impingement angle of the vapor plume has also been observed to disrupt the powder bed<sup>[43,44]</sup>. The vapor plume shape determined by its relative direction to the shielding gas flow can also possibly affect the oxidation and reduction characteristics<sup>[45]</sup>. Consequently, the oxidation characteristics would affect the melt pool dynamics and part quality due to the level of oxygen content. The vapor plume that forms under different process parameters also results in different spatter characteristics, which have been identified to cause defects in AM parts. The control of beam parameters, such as laser defocus<sup>[46]</sup> or beam diameter<sup>[47]</sup>, can also be used to reduce the build time. The control of shielding gas parameters is also essential to ensure the proper removal of by-products while preventing disruption to the powder bed<sup>[48,49]</sup>.

In addition, other methods for grain refinement exist, such as ultrasound<sup>[50,51]</sup>, the direct introduction of nanoparticles for inoculation<sup>[52–58]</sup> and the introduction of carbon nanotubes for grain refinement and reinforcement<sup>[59–61]</sup>. Magnetic fields can also be used to control the solidification behavior and microstructure formation<sup>[62,63]</sup>. Essentially, the number of parameters that can be controlled in an AM system could increase indefinitely as the technology develops. Nevertheless, increasing our knowledge regarding the processing allows us to introduce additional control measures to potentially reduce the variability and uncertainty that are rampant across AM systems. For example, the fact that many studies do not include the effect of varying layer

thickness, chamber processing conditions (direction of scan and speed flow), spreader velocity *etc.*, already accounts for a significant variation observed across different machines, despite using the same process parameters. The optimal parameters determined for one alloy system may change depending on the machine used, the lifetime of the machine, its geographical location *etc.*, and these effects remain unknown.

In contrast, in metal AM processes that do not utilize localized heat sources during processing, problems arising from residual stress can be avoided. BJ is one such unique metal AM technique, where the fusion of a material occurs separately. However, problems related to powder-based processes remain in BJ and crucial effects related to the binding and debinding process arise. Instead of the instantaneous heat input during manufacturing, the main process parameters are the fluid properties of the binding agent governing droplet breakup and adhesion, binder-powder compatibility, binder saturation and curing parameters (time and temperature) [64–66]. As BJ is different from the aforementioned AM processes, the mechanisms are not elaborated in detail here as it is not the focus of this review. Nonetheless, the discussions of the optimization framework in finding optimal process parameters remain relevant.

Therefore, for any processing technique, it is of utmost importance to understand the formation mechanisms of defects or other process phenomena and subsequently identify the process parameters that can influence these formation mechanisms. In PBF or DED, the process parameters fundamentally dictate the thermal input to the material, effectively influencing the melt pool dimensions, solidification characteristics and thermal history. The microstructural evolution, defects and mechanical properties are correspondingly affected. Hence, *any* parameter that influences the conditions for thermal input and material behavior is a potential process parameter and therefore many process parameters can naturally be identified. For example, in the PBF process, the parameters, mechanisms and defects can be categorized as shown in Figure 1 (with reference to Sun *et al.* [67]). Similar process-mechanism-defect relations have been summarized by Svetlizky *et al.* for DED processes and Li *et al.* for BJ processes [7,66].

## OPTIMAL PROCESSING WINDOW

Given the plethora of parameters that can be identified during the AM process, a direct treatment of this multivariate problem is impractical. Instead, key objectives and parameters are identified to simplify the problem. The key objectives are defined by quantifiable physical metrics at various scales, such as physical conditions (melt pool modes and aspect ratios), defects (relative density, porosity and distortion tolerance), mechanical properties (surface roughness and tensile and fatigue properties), microstructural properties (grain phases, grain size, grain aspect ratio, grain boundary angle and grain misorientation) or manufacturing performance (time, energy, cost and efficiency). In contrast, the key parameters are controllable process parameters limited by the capability and customizability of the machine. Owing to the complex metallurgical process that occurs during AM, the key parameters may be identified simply by the consideration of bulk energy input during the process. In particular, the influences of the heat power ( $P$ ), scanning velocity ( $v$ ), hatch spacing ( $h$ ) and layer thickness ( $t$ ) on the AM part quality are most commonly investigated in PBF. These four parameters are commonly characterized as a volumetric energy density (VED) [5]. In addition to VED, other parameter combinations have been proposed, such as linear input energy density, linear energy density and surface energy density [67]. Although VED is a common method for characterizing the energy input, it has been shown to be unreliable due to the overt physical simplification.

Across the literature, the most common method to characterize the energy input in the AM process is VED. Its prevalence is partly due to early efforts that focused on optimizing part porosity, which VED provided sufficient prediction for. However, while simple bulk energy considerations, such as VED, are easier to quantify and are heavily used in most experiments, they fail to accurately capture the effects from complex physical phenomena in AM [74,75]. Therefore, VED may be able to provide an aggregate prediction of the porosity

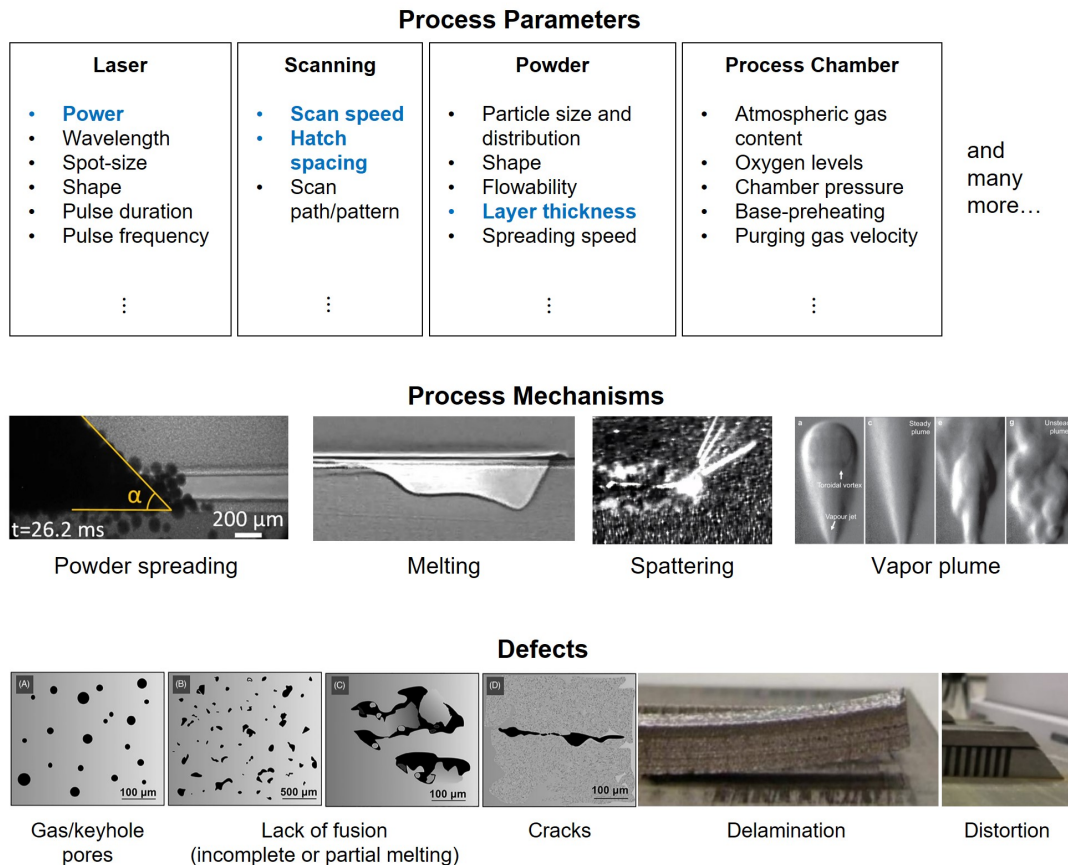


**Figure 1.** Process parameters in the PBF process, which affect the process mechanisms and defect formation in AM. DED processes also share similar defects, though the formation mechanisms may differ slightly. Illustrated here are the uncovered mechanisms for PBF, which include powder spreading [68], melting [69], spattering [43] and vapor plume [70]. The defects range from gas, keyhole pores, lack of fusion pores to cracks [71], delamination [72] and distortion [73].

but not the mechanical properties [11]. As the parameters do not correlate strictly in a linear fashion, direct comparisons by VED only could be misleading [16]. In fact, different parameter combinations with the same VED values could yield different mechanical properties. For example, Greco *et al.* showed that the SLM of stainless steel parts under the same VED yielded different microhardness characteristics [76]. The simplified VED consideration ignores the crucial transient dynamic effects, particularly the thermal history that governs both the evolution of the microstructures and the effect of distortion by the residual stresses.

Despite the limitations of using VED, it remains a popular option as it provides a semi-quantitative comparison for basic analysis and comparison between different process parameters. Research has focused on the influence on these key parameters in AM due to the simple quantification. It is generally observed from the multitude of studies in metal-based AM, as well as the studies in laser-based fusion welding, that laser power has the most significant effect, followed by the laser scan velocity [77,78]. Further evidence of laser power being a more dominant process parameter is seen in the derived parameters, such as the normalized enthalpy parameter [79] and the dimensionless “keyhole” parameter [80] to determine the keyhole mode transition. There is currently no de-facto parameter that is able to universally characterize the AM process, as identified by the ASMC research gap. Regardless, these four main parameters alone already have competing influence with one another on the key objectives, such as the melt pool dimensions, porosity and microstructure.

Similar to the welding process, in the PBF and DED processes, the mode is primarily differentiated into the heat

conduction and keyhole modes<sup>[81,82]</sup>. It is possible to characterize the modes in AM by considering a simple thermal model and the application of the non-dimensionality of processing variables. Usually, if the laser power is too low and the scanning velocity is too high, lack of fusion occurs and a complete print is not obtained. In contrast, the keyhole mode in the PBF process is generally avoided as it introduces keyhole porosities through the collapse of the keyhole<sup>[79,83,84]</sup>. As such, there is a “Goldilocks” zone where a suitable power and velocity combination can be obtained. However, the notion that the keyhole mode is necessarily undesirable may not be equivocal. In fact, experiments suggest that a power-velocity combination that corresponds to a stable keyhole mode may be beneficial. Scime and Beuth<sup>[85]</sup> examined the cross-sectional morphology of melt pools processed under the keyhole regime and found that the occurrence of keyhole porosities was infrequent. Works by Zhao *et al.* also suggest that the existence of a stable keyhole regime is possible<sup>[69,86]</sup>. Indeed, a stable keyhole with no keyhole porosities arising from keyhole collapse would be ideal given its deeper penetration, which theoretically would allow for a larger layer thickness and shorter build time. Still, the keyhole mode is still generally avoided as the stochastic nature of the keyhole fluctuation is difficult to exactly predict and control. In contrast, Jadhav *et al.* demonstrated that the keyhole mode may be favorable for metals and alloys with high conductivity, such as copper<sup>[87]</sup>. Under these conditions, metals with high conductivity are able to conduct heat away rapidly before the unstable keyhole collapses, thereby avoiding pore formation.

In addition to changes in the melt pool dimensions, process parameters have a more fundamental impact on the microstructure of the material. The rapid heating and cooling cycles in AM are characteristic of the AM process. Rapid cooling rates of  $10^5 - 10^7 K \cdot s^{-1}$  and correspondingly high-temperature gradients  $10^6 - 10^7 K \cdot m^{-1}$  have been reported for PBF processes<sup>[88]</sup>. Due to rapid solidification, the microstructures formed are generally a mix of equiaxed or epitaxial crystals at the periphery and dendritic along the scan direction<sup>[89]</sup> [Figure 2]. Notably, some process parameters have been identified to have a direct influence on grain morphology. For example, in 17-PH stainless steel, the laser power and scanning velocity directly influence the austenitic grain size<sup>[77]</sup>. In fact, by careful adjustment of the process parameters (power and velocity),  $\langle 011 \rangle$  grains can be produced in stainless steel, which can simultaneously improve the ductility and strength of steel, thereby overcoming the conventional trade-off between these two properties<sup>[90]</sup>. Interestingly, a lamellar microstructure with alternating  $\langle 100 \rangle$  and  $\langle 110 \rangle$  grains can be obtained solely by the control of process parameters alone<sup>[91]</sup>.

Similarly, the beam shape of the laser can be designed to alter the microstructure formation. For example, Roehling *et al.* demonstrated that the use of elliptical beam shape can improve the mechanical properties of the printed part<sup>[92]</sup>. The solidification direction in AM is highly directional. As the crystallization occurs in a preferential direction during the AM process, it is also common for AM parts to exhibit anisotropic properties<sup>[93]</sup>. Due to overlaps, the remelting of the overlapping regions between the melt pool creates new microstructural textures and features that cannot be achieved through conventional manufacturing<sup>[94]</sup>, such as spiralling microstructures<sup>[95]</sup>, lamellar grains in SS316L<sup>[91]</sup> or duplex microstructures in Ti-6Al-4V<sup>[96]</sup> [Figure 2C-F]. In this regard, the metal microstructure can be directly controlled through the adjustment of the process parameters, which is indirectly the objective of many studies attempting to optimize the mechanical properties. Due to the unique microstructures in AM, some alloys manufactured via AM have comparable or superior mechanical strength compared to their conventionally manufactured counterparts (such as casting or wrought)<sup>[12,97-103]</sup> [Figure 2E-F]. However, this rapid heating and cooling process generates high residual stresses in metal AM during fabrication, which may lead to warpage and cracking<sup>[19]</sup>. Moreover, due to the prevalence of pores in metal-based AM, the fatigue performance of AM components is generally poorer than parts manufactured through conventional means<sup>[104,105]</sup>.

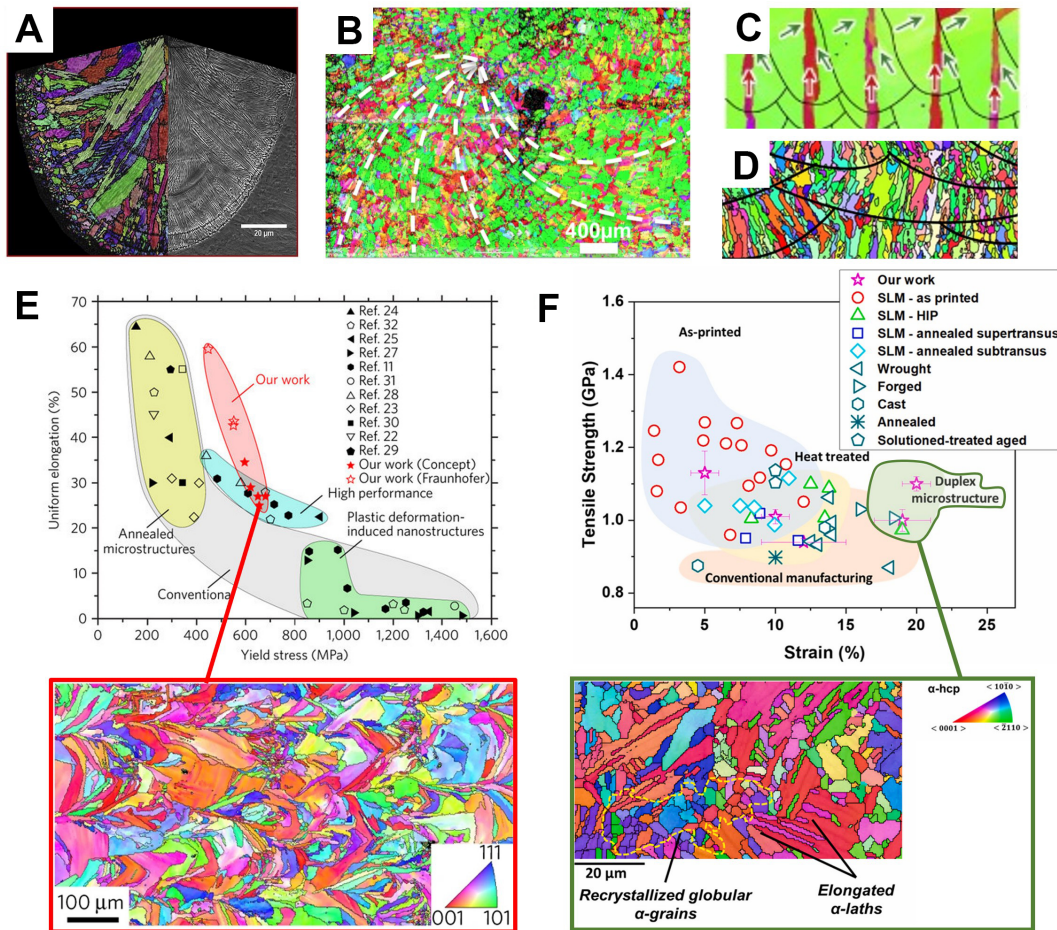


**Figure 2.** Microstructures and mechanical properties in AM. (A) Microstructure of a melt pool, equiaxed at the periphery and dendritic along the solidification direction [89]. (B) Spiral microstructure pattern observed due to 67 degree layer rotation scanning strategy [95]. (C) Lamellar grains comprised of alternating  $\langle 100 \rangle$  and  $\langle 110 \rangle$  grains in stainless steel 316L by altering laser power and scanning speed [91]. (D) Preferred nucleation of  $\langle 110 \rangle$  grains in stainless steel 316L [90]. (E) AM SS316L has a good combination of uniform elongation and yield stress compared to conventionally manufactured counterparts [99] and its corresponding microstructure. (F) AM Ti-6Al-4V with duplex  $\alpha$ -grains and  $\alpha$ -laths, enabled by the deliberate introduction of pores, followed by hot isostatic pressing [96].

Given the conflicting objectives presented in both the melt pool dimensions and microstructure, most studies have defined an optimal processing window for AM materials, obtained mostly through experiments. The notion of a processing window for laser processing is a common strategy, as explained and expanded by Ion *et al.* [106]. In AM, the processing map methodology has been proposed as early as 2001 [107] and applied to different materials [108]. Processing windows are often presented as a surface contour plot of the design criteria with power and velocity in the main axes, with the critical lines differentiating the processing regimes [Figure 3A]. The optimal processing window approximately quantifies the relation between the input parameters and output objectives and provides a visualization and guideline to achieve the desired objectives. Within such a window, a combination of process parameters can be suggested to avoid undesirable defects induced by key-hole modes or improve melt pool adhesion [109]. Moreover, the printability of new alloys can also be assessed via the processing map methodology. Johnson *et al.* performed simulations and experiments to generate the process map for Ni-5 wt.%Nb and the CoCrFeMnNi high entropy alloy [110]. However, the authors highlighted the importance of the quantification of uncertainty to outline the boundaries of printability.

In contrast, normalized process diagrams [107,111] have also been proposed to narrow the processing region for prediction in the early research of new alloys [Figure 3B]. The effect of the process parameters may be

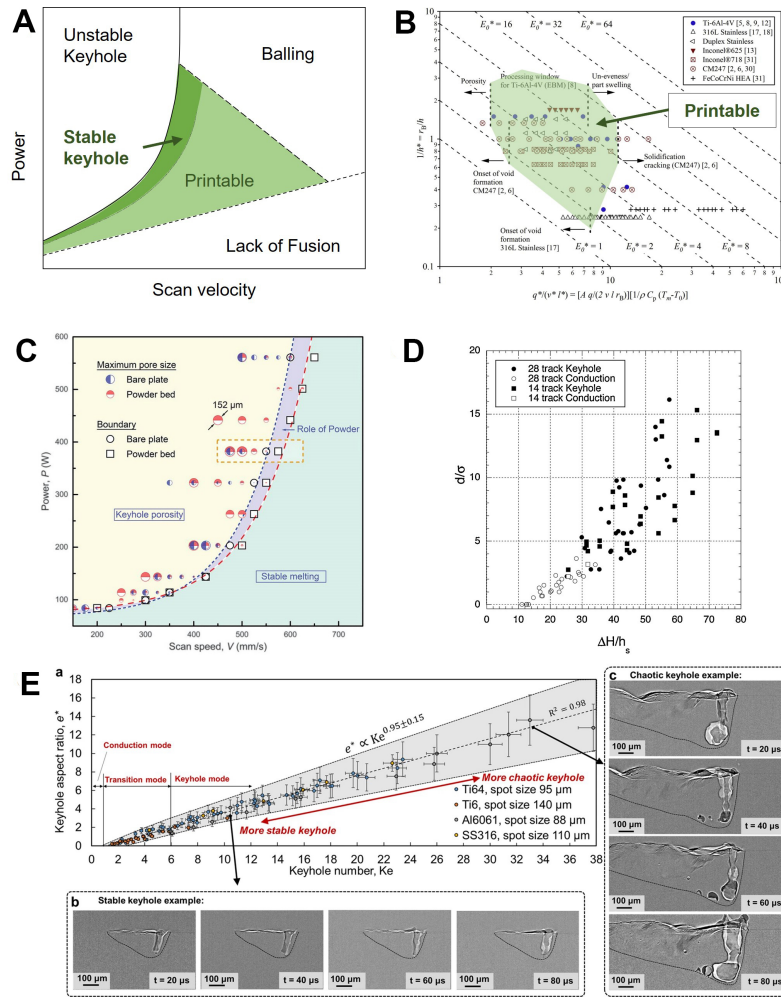


**Figure 3.** Processing maps in AM. (A) Conventional processing map for defect-free print represented by laser power and scan velocity as the two main axes. It consists of four regions: keyholing; balling; lack of fusion; printable region. A stable keyhole may be optimal for the build rate and part quality. (B) Normalized process diagrams [111] to evaluate the printability of different alloys based on material properties and enthalpy input. (C) Keyhole process diagram [69] that describes the boundary where the keyhole becomes unstable. (D) Normalized enthalpy [79] to delineate the regions between conduction and keyhole modes in AM. (E) Universal scaling law for keyholes [80] to describe the stability and variability of a keyhole based on a 'keyhole number'.

estimated by comparing with energy input to the material properties. In fact, the use of non-dimensional maps or parameters may shed light on certain universal characteristics of AM, which are not immediately observable from the raw data alone. Such “scaling laws” could be derived, such as a scaling of melt pool dimensions [112] and the differentiation of conduction and keyhole modes in AM [79,80,113] [Figure 3C-E]. These examples further suggest the potential of using other dimensionless parameters in AM [114–116] to aid the characterization and identification of suitable processing regions during the early stages of research for new AM alloys, thereby alleviating the experimental burden. For example, dimensionless parameters could be used to estimate the effects of thermal distortion and chemical composition [117].

It would be prudent to consider analytical and non-dimensional approaches for early process map generation. Thereafter, simulations combined with experiments can be used to further refine the search directions within the process space to more accurately deduce the specific points for printing. For example, Tang *et al.* used the analytical Rosenthal solution and assumed an elliptical geometry to estimate the lack of fusion defects and predict the porosity under different energy densities [118]. Gordon *et al.* built on this concept by considering the keyhole boundary predicted by the drilling velocities to propose a “defect structure property map” [119]. Zhang

*et al.* proposed a practical framework by reducing the theoretically infinite search space to a finite region with upper and lower bounds using the Eagar-Tsai thermal model<sup>[120]</sup>. The printability map was then calibrated via Bayesian statistical modeling with single-track experiments. However, the elliptical criteria adopted by the three aforementioned studies are arguably over-simplified, though they are sufficient for regions where the conduction mode is encountered for rough mapping purposes<sup>[118–120]</sup>.

Moreover, most optimization processes consider the parameters to be constant. This may not be true as a level of uncertainty exists during the printing process. While uncertainty analysis methods can be applied, there are some parameters that have been evaluated in detail. For example, it is well known that the effective layer thickness changes during printing and reaches a steady state<sup>[121–123]</sup>, different from its nominal (user-set) powder thickness. Such a phenomenon occurs due to the powder packing density and material consolidation during each deposition<sup>[123]</sup>. Hence, processing windows should ideally take into account such effects for optimization, as suggested and demonstrated by Ahn *et al.*<sup>[124]</sup>. This example suggests that optimized parameters may differ between the initial stage and steady-state stage of printing and the assumption that parameters are “constant” is only applicable when a quasi-steady-state process has been achieved.

Finally, the optimization of process parameters in AM must be context specific. For instance, the minimization of pores need not be a necessary goal. From a traditional engineering perspective, better material properties in metals can be achieved with minimum porosity (densification). Thus, most work in metal AM is devoted to identifying processing regions with minimum porosity, which usually corresponds to improved fatigue<sup>[125]</sup> and corrosion properties<sup>[126,127]</sup> for AM parts. However, pores can be deliberately introduced and exploited to improve mechanical properties. Bustillos *et al.* demonstrated a microstructural engineering approach, in which they deliberately processed Ti6-Al-4V with a lack of fusion defects and subsequently used hot isostatic pressing to ‘heal’ such defects<sup>[96]</sup>. Through this approach, an unprecedented strength and ductility combination for Ti6-Al-4V was achieved. This study demonstrates that the traditional notion of the ‘optimal processing region’ in AM need not be the region with minimal porosity. Deliberate porosity engineering may provide an alternative in AM processing, which on a larger scale, corresponds to lattice design<sup>[128]</sup>.

Moreover, the optimal process parameters for one property of interest do not necessarily translate to other properties. For example, Gong *et al.* showed that different optimal process parameters are obtained to achieve maximized tensile strength, hardness and fatigue resistance in Ti-6Al-4V<sup>[14]</sup>. Therefore, the AM practitioner should then prioritize the manufacturing objectives based on the application requirements and select a suitable process parameter combination. A further discussion of the formal definition of such an optimization problem is included below. On this note, in certain scenarios, maximizing the mechanical properties is not the goal. For example, it is a traditional notion that the surface roughness of AM parts should be minimized for better fatigue properties. This is applicable for applications in the aerospace<sup>[129]</sup> and automotive<sup>[130]</sup> industries, where structural efficiency and integrity are key. However, in the production of medical implants, a higher surface roughness is desired for osteogenesis, while the mechanical properties are not maximized but tailored to match the bone<sup>[131]</sup>. In contrast, for orthodontic applications, the fabrication of customized brackets requires minimal distortion and porosity<sup>[132]</sup>. These studies demonstrate that optimization problems are always context specific and reinforce the need for robust PSP models for multi-objective optimization problems to be feasible.

In summary, the control of process parameters is directly linked to the part quality, as the parameters influence the physics during processing. The poor selection of process parameters will result in poorly fabricated parts and wasted time, materials and energy. Traditionally, the optimal parameters refer to densification of the parts. Yet, in certain applications, we may want to tailor the desired outputs that may not correspond to the highest strength or ductility of the part. Hence, optimal process parameters have to be determined for the application objectives.

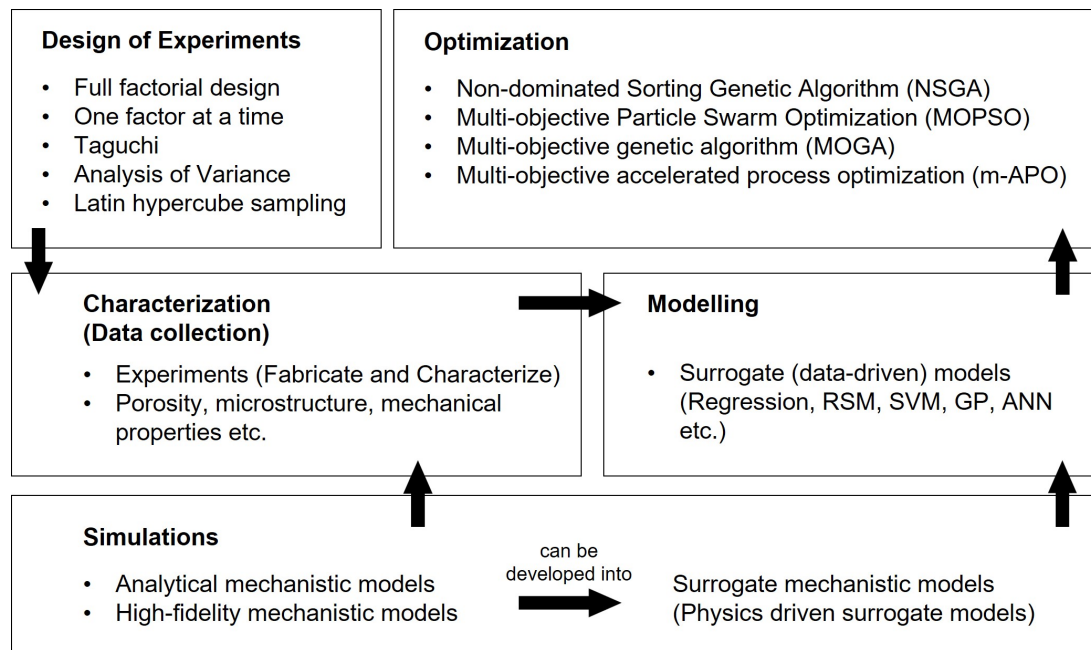


**Figure 4.** Optimization framework in AM summarized into four sections: design of experiments; characterization; modelling; optimization. Numerical simulations can support the characterization (sampling of process space) and modelling aspects of optimization.

## OPTIMIZATION FRAMEWORKS IN AM

In the discussion of the optimization of process parameters in AM, we may distinguish the approach into two main phases. The first phase is to determine the optimal process parameters for a defect-free window. This is commonly quantified by the part porosity or the relative density of the AM part. The second phase is the refinement within such a window and involves identifying the specific process parameter combination that is able to meet, or even exceed, the requirements of the AM user. Often the influence of process parameters on the goals and part performance are conflicting. As such, the optimization of parameters in AM to meet user-defined objectives is effectively a multi-objective optimization problem.

Optimization frameworks in AM can be systematically summarized to comprise four main sections: DoE; characterization (data collection); modelling; optimization [Figure 4]. DoE methods describe strategies to sample the process space for investigation. These sampling points are then characterized, which in AM include the porosity, microstructure and mechanical properties, which have been the focus of the past decade. The data collection is followed by a surrogate modelling of the input-output relations, such as regression, response surface modelling (RSM), Kriging, support vector machines (SVM) and artificial neural networks. Subsequently, an optimization algorithm, such as gradient descent, Pareto search, particle swarm optimization and evolutionary algorithms, are used to locate the minima points. Under such a framework, the process-structure-property relations (and their inverse) can be approximated.

In fact, most processing maps have been obtained in this manner. Early efforts at optimizing process parameters for AM were largely experimental, focusing on the material characterization. This experimental research in metal AM has largely followed the sequential progress (process characterization, modelling, improvement, monitoring and comparison and finally process reliability) described and detailed in the Engineering Statistics Handbook by the National Institute of Standards and Technology (NIST)<sup>[133]</sup>. Thereafter, the data obtained from experiments are fitted with classical response surface models or regression (which strictly speaking, are surrogate models). Note that the data acquisition for modelling need not be experimental; if sufficiently rigorous mechanistic models are developed, analytical or numerical models can be employed to sample the pro-

**Table 1. Process parameter optimization studies on different materials and the methods used**

Optimization method	AM technique	Material	Optimization problem and study	Ref.
Taguchi and ANOVA	SLM	Ti6Al4V	Porosity	[134]
Full factorial DoE	SLM	Invar36 and SS316L	Density, tensile strength and Fracture	[82]
Basic study of few parameters	SLM	Inconel 718	Surface roughness and fatigue life	[125]
Full Factorial DoE and regression	SLM	Invar36 and SS316L	Density, tensile, fracture	[135]
Full factorial DoE and regression	SLM	AlSi10Mg	Microstructure, high cycle fatigue and fracture	[104]
Full factorial DoE and regression	SLM and SEBM	Ti4Al4V	Density, tensile, fatigue	[14]
Full factorial DoE and regression	SLM	Iron-based powders	Balling (density)	[29]
Full factorial DoE and regression	SLM	SS316L	Roughness	[136]
Full factorial DoE and regression	SEBM	SS316L	Tensile strength and relative density	[137]
Full factorial DoE and regression	SLM	Ti6Al4V	Melt pool dimensions	[138]
factorial design	SLM	Maraging steel	Relative density	[139]
Full factorial DoE	SLM	Ti6Al4V	Porosity	[16]
Full factorial DoE	SLM and EBM	Ti6Al4V	Porosity	[140]
RSM with ANOVA	DED	Ti-15Mo	Melt pool dimensions	[141]
RSM with ANOVA	SLM	Ti6Al4V	Elastic modulus, surface roughness, ultimate compressive strength, porosity	[131]
Full factorial DoE	SLM	SS316L	Tensile strength	[142]
Full factorial DoE	SLM	Martensitic CX SS	Surface roughness and relative density	[143]
RSM	SLM	Ti6Al4V	Surface roughness	[144]
Taguchi and ANOVA	BJ	SS316L	Transverse rupture strength	[145]
Taguchi and ANOVA	BJ	SS420	Surface roughness and dimensional accuracy	[146]

cessing space. Therefore, AM models at different length scales could replace experiments (digital twins) in sampling the process space for optimization purposes.

### Design of experiments and characterization

In the NIST handbook, the DoE is described in the section “Process Improvement”. Parametric studies were implemented in the earlier stages of AM research when the main focus was to create fully dense parts and reduce part porosity. In AM, early parametric studies of the process parameters utilized DoE methods that include full factorial design, Taguchi and so on, which sampled the process space for investigation, followed by analysis with the analysis of variance (ANOVA) and RSM. Some of the methods used in parametric studies are tabulated in [Table 1](#).

In [Table 1](#), the most common method is a  $L$ -level,  $k$ -factor full factorial design method. Usually,  $k = 2$  factors (power and scanning speed for laser-based methods or current and scanning speed for electron beam-based methods), while  $L$  varies when no specific statistical method is specified. This is the most basic method, where the full range of process parameters at different levels separated at constant intervals is studied. For example, in a study of the influence of processing parameters on the density and mechanical properties of Invar36 and 316L stainless steel [135], three different levels of laser power (200–300 W), scanning velocity (600–1000 mm/s) and hatch spacing (0.08–0.12 mm) were investigated. Evidently, the full factorial method is straightforward, easy to implement and commonly used when there is no prior information on the material properties and no expectation of the outcome.

However, this method is time consuming and inefficient due to the exponential increase in experiments required for each increase in interval (commonly described as the “curse of dimensionality” [147]). For example, in the same aforementioned study of Invar36 and 316L stainless steel [135], simply having  $k = 3$  factors at  $L = 3$  different levels required  $N = L^k = 3^3 = 27$  samples. As the interval of the studied parameters is usually large, the result obtained from a full factorial experimental study usually has low resolution, requiring regression models to fit the data.

Experiments in AM are costly due to both the material cost of the powder and the operational cost of keeping the AM machine on for extended periods of time [148]. More importantly, experimental characterization can be time consuming. Therefore, it is important to conduct the lowest number of experiments possible while extracting the maximum amount of information from the number of samples available. As such, statistical methods are used to significantly reduce the number of experiments while maintaining the range of study. Common methods in AM include orthogonal, fractional factorial and Taguchi’s (parameter) method, ana-

lyzed with ANOVA and RSM. Such methods are also commonly found in other engineering applications. In a parametric optimization study for Ti6Al4V<sup>[134]</sup>, the application of Taguchi's method allowed the researchers to obtain the optimal combination with 16 samples via ANOVA and signal-to-noise ratio considerations. Statistical methods and analysis can therefore aid experimentalists to reduce the number of experiments to obtain the optimal processing parameters. Simultaneously, it is common that a surrogate model can also be obtained with regression methods, such as the polynomial surface response methodology (e.g., RSM). Response surface methodologies are easy to implement and cost-effective. In a study of the optimization of Ti-6Al-4V, Elsayed *et al.* demonstrated that the output responses of surface roughness, porosity, elastic modulus and compressive strength due to three inputs can be modelled with the use of only 17 samples<sup>[131]</sup>. Similarly, the corrosion properties of AM high entropy alloys can also be optimized using RSM<sup>[149]</sup>. Data-driven methods are sensitive to data uncertainty since they rely on the accuracy of the data.

However, as each experiment uses a different AM machine and powder, the results cannot be easily translated and compared with one another. Even if the same machine and same process parameters are used, the results may not be consistently reproducible<sup>[150]</sup>. On this basis, it was demonstrated that data from previous studies can be utilized for current optimization problems despite having different processing equipment and materials. This can be achieved by generalization of the sequential minimum energy design method and characterizing the difference in responses between prior and current studies as a probability distribution. Using this method, the authors showed that an optimal combination of parameters can be obtained with just five experiments<sup>[151]</sup>.

Regardless of the current limitations of experimental methods, experimental optimization will remain the first go-to method for empirical observation, especially for the characterization of new alloys. However, with the development of simulation capabilities, it presents a possibility where we can predict and design new alloys via simulations, which can be subsequently validated with experiments instead of performing trial-and-error characterization.

### Modelling for optimization

Current modelling efforts in the optimization of AM process parameters are summarized in [Figure 5](#). The optimization of AM process parameters requires a relation from the processing inputs to outputs. Earlier, we elaborated that experiments have worked towards this objective by classical methods via RSM or regression via VED. Such efforts are, strictly speaking, simple data-driven surrogate models. However, such models can only provide approximations due to oversimplified parameters. Therefore, a deeper understanding and modelling of the PSP relations are necessary for a more adequate description of AM part quality from its process parameters, for example, through the efforts of mechanistic modelling. Mechanistic modelling efforts at multiple length scales in AM can thus provide the input-output relation needed for optimization purposes. However, current mechanistic models still incur relatively high computational costs, which render them unfeasible for optimization studies. Hence, other more sophisticated data-driven approaches, such as Kriging, SVM, GP, NN and so on, have since been applied in AM, which have gained tremendous interest for the precipitation and resurgence of the field of ML. Nonetheless, these data-driven models are often criticized for being “black-box” models without a physical basis. Here, as we discuss the validity of applying these models for optimization in AM, we find that the crucial link is creating appropriate surrogate models derived from mechanistic models.

#### *Mechanistic modelling*

Like most metallurgical problems, it is almost impossible to derive *a priori* information from first principles due to the multi-scale multi-physics interaction in the AM process. Understanding the PSP relationship in AM remains a daunting task, although the physical mechanisms from the nanoscale (e.g., twinning and nano-oxides), microscale (e.g., fish-scale microstructure and columnar-equiaxed transition) and mesoscale (e.g., powder bed dynamics, melt pool dynamics and vapor plume) have been increasingly clarified over the years with experiments and simulations. Experimental characterization of the AM process is highly challenging due

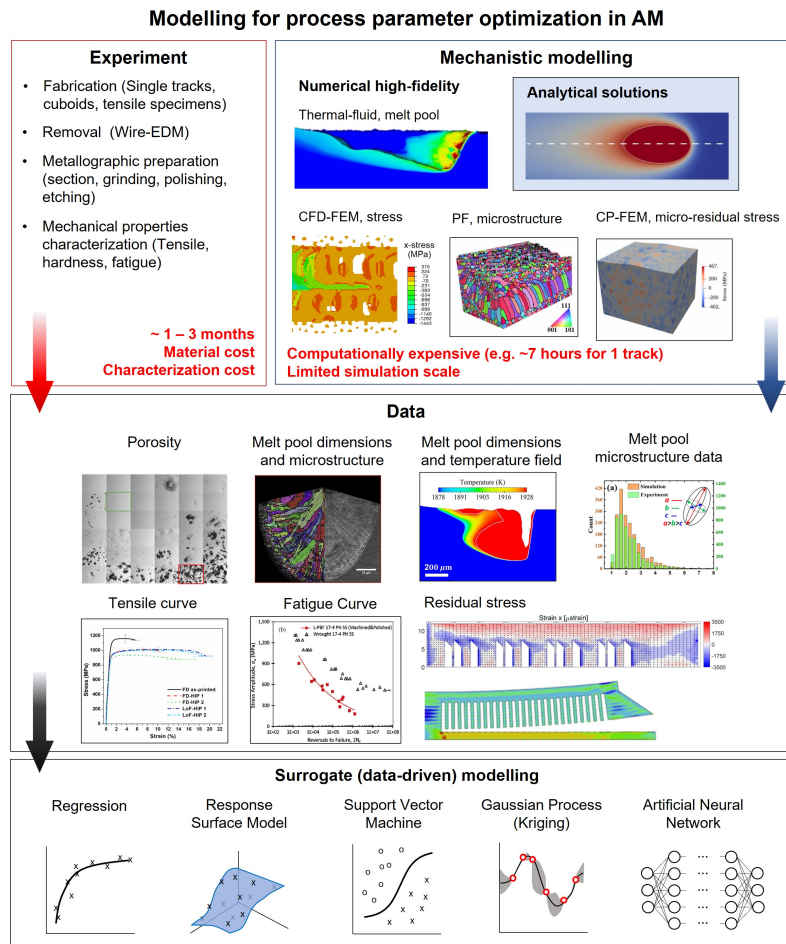


**Figure 5.** Modelling for optimization in AM. The process map in AM has mostly been characterized using experiments, which are costly. Analytical models (e.g. Rosenthal's solution [152]) provide rapid prediction of the process map but become inaccurate when convection effects are significant. High-fidelity models (e.g. thermal-fluid melt pool simulations for melt pool [153], novel computational fluid dynamics and finite element model (CFD-DEM) coupling for stress prediction [23], phase field (PF) models for microstructure [154] and crystal plasticity and finite element model coupling (CP-FEM) for micro-residual stresses [155]) can account for such complex physics but have limited simulation scale. Data generated from experiments include porosity [96], melt pool dimensions and microstructure [89], tensile characteristics [96] and fatigue characteristics [156]. Similarly, simulations can generate data such as melt pool dimensions and the temperature field [35], melt pool microstructure data [154] and residual stresses [157,158]. The data generated by these models can be further analyzed with data-driven algorithms to generate surrogate models to generate the response maps.

to the extremely short time scales that occur from the rapid solidification rates in AM. Currently, state-of-the-art experimental characterization of the melting process uses high-speed imaging to capture the melting process and its dynamic interaction with the powder bed, such as powder spattering and denudation induced by the vapor plume [43]. Importantly, the use of in-situ operando X-ray synchrotrons has revealed many crucial information, such as the keyhole dynamics, its instability and pore formation [69], and effects of nanoparticle additions [159]. Moreover, the combination of Schlieren imaging and in-situ x-ray operando imaging provides a simultaneous observation of the AM process and reveals the interaction between the vapor plume and melting process [70]. However, these experiments require specialized equipment, are challenging to perform and only provide two-dimensional information (cross-sectional). Three-dimensional interactions may not be thoroughly captured.

Hence, mechanistic modelling through analytical or numerical simulations can aid researchers in probing the physical interactions during the AM process by increasing the accessibility to investigate underlying phe-

nomena at shorter time scales. Such models and their descriptions have already been reviewed by various authors<sup>[160–162]</sup>. Therefore, a review of mechanistic models will not be repeated here. Instead, the applicability of these models for optimization applications is discussed.

The mechanistic modelling of AM across different length scales is an active area of research. For the purposes of optimization, we can distinguish mechanistic models into analytical, numerical and semi-analytical models. Most modelling in AM has focused on the mesoscale, i.e., the melt pool. At this scale, analytical models are computationally inexpensive. These models are borrowed from laser welding research, which are variants of Rosenthal's solution, such as Rylakin's model, Eagar-Tsai's model and so on. However, these models are only applicable in the conduction regime as the models assume pure conduction; when melt pool convection becomes significant, the prediction will deviate from actual case<sup>[163]</sup>. Such analytical models also fail to predict the volatile nature of the keyhole.

In contrast, validated numerical models offer greater accuracy. FEMs are the only practical models used for part-scale modeling and simulation. Non-FEMs at the part scale have also been developed, for example, Yang *et al.* proposed a physically-based PSP model for process parameter optimization of Ti6Al4V with a focus on the mechanical property prediction of yield strength, flow stress and strain hardening<sup>[164]</sup>. However, part-scale models are unable to provide accurate temperature fields at the melt pool level as they ignore fluid dynamic effects. High-fidelity models that incorporate the fluid dynamic effects<sup>[35,165,166]</sup> (usually CFD models) are able to capture the effect of Marangoni convections widening or deepening the melt pool, evaporation, advection of materials and the effects of vapor plume. However, such models are computationally costly and have limited simulation scale. Although high-fidelity mechanistic models are able to accurately predict PSP relations, they are limited by their exorbitant computationally requirements that are prohibitive. Realistically, high-fidelity models cannot be used for multi-objective optimizations as it is computationally intractable to sample the process space directly. Therefore, only analytical mechanistic models have been used to sample the process space for the identification of processing regions and optimization purposes.

However, mechanistic models can still serve as the foundation for the development of physics-based surrogates, which can then sample the process space with less computational time. Moreover, it is frequently espoused that the study of single tracks via experiments and simulations could reveal crucial dynamics to aid in process improvement. However, the use of single-track results must undergo calibration to reflect results at the part level, as the missing link is the effect of thermal history and dissipation. Hence, such a link would be desirable if single-track results are used for the prediction of the part-scale properties.

#### *Surrogate modelling*

Surrogate models, as the name implies, are not true descriptors of the physical mechanisms that occur but are sufficiently descriptive for engineering applications<sup>[167]</sup>. Surrogate models can be developed to approximate the mechanistic models or can have no physical basis and used as-is, even when the physics of the AM process are not fully known (black-box). For example, the early use of regression and quantification via VED is the simplest surrogate model<sup>[136]</sup> [Figure 6]. More frequently, the RSM is adopted to illustrate the output response surface due to laser power and scanning velocity. However, there is a growing trend to use more sophisticated data-driven algorithms, i.e., ML, to directly predict the output response from process parameter inputs.

The use of ML in AM is a burgeoning area of research (beginning circa 2016) and has been made possible due to two main reasons. Firstly, there has been a recent surge of interest and hype in ML-based research since 2010. This has resulted in a myriad of free-access and easy-to-use open-source algorithms and programs for anyone to use in any application. Secondly, an enormous amount of data in AM has been generated from experiments and simulations for the past two decades. Therefore, it is natural and practical that ML is applied to AM optimization due to the availability of both algorithms and databases. This allows optimization in AM to

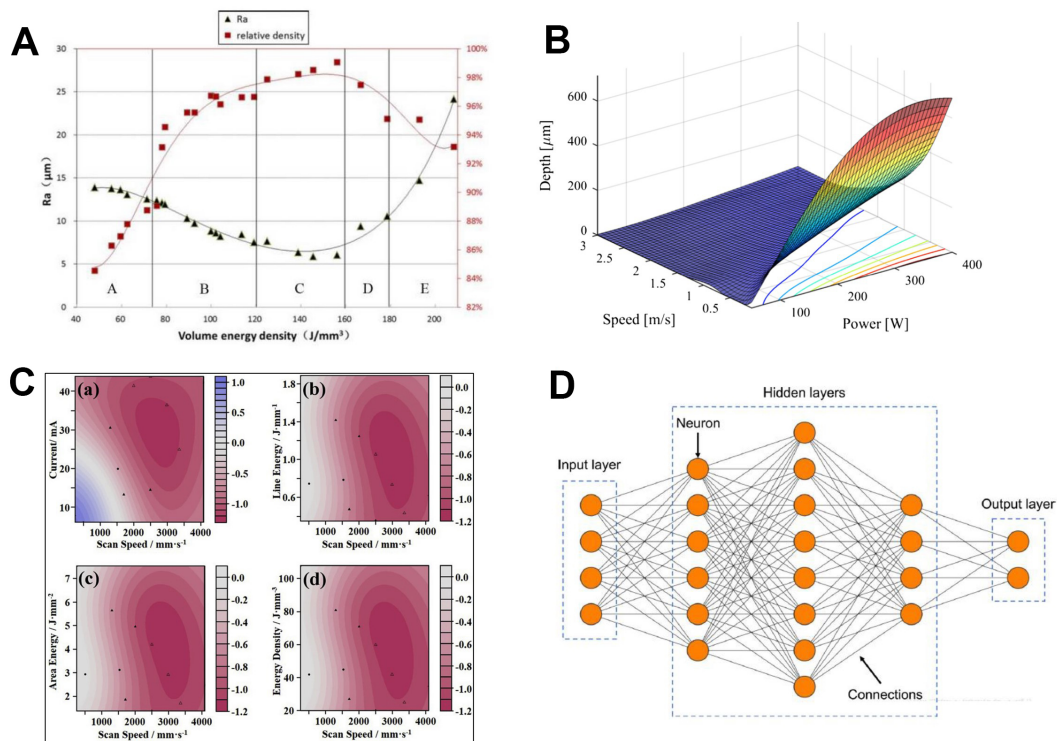


**Figure 6.** Surrogate models to describe the response output. (A) Surface roughness and porosity described using regression via VED parameter [136]. (B) Response surface obtained with Gaussian process modelling [168]. (C) Process maps generated using support vector machine [169]. (D) Schematic of a neural network (obtained from Wang *et al.* [170]).

be conducted resourcefully in a cost-effective manner provided the researcher has access to past data. Recent reviews on the ML methods applied in AM have listed and elaborated comprehensively on the multiple applications of ML in metal AM, such as process planning, parameter optimization, geometric sensing and control, defect detection and mitigation, quality prediction and assessment, cost estimation and data simplification for analysis [170–172]. In this section, only the methods used in process parameter optimization are discussed. Similar to the experimental methods discussed earlier, ML methods applied in process parameter optimization are largely focused on obtaining a processing map of zero-defect manufacturing. For example, Yeung *et al.* used neighboring-effect modelling to optimize the scan strategy [173]. Wang *et al.* used a two-level data-driven surrogate model to perform a process optimization under uncertainty with equiaxed grains as the optimization objective [174]. Mondal *et al.* used a hybrid data-driven method to predict the melt pool dimensions via a low-cost Gaussian process (GP) surrogate model developed from an experimentally validated analytical three-dimensional model [175]. Narayana *et al.* used an ANN to generate process maps for the optimization of build height and density [176]. Nguyen *et al.* setup an ANN to minimize the porosity Ti6Al4V [177]. These methods, including GP regression models, ANNs, random forest networks and regression Trees, are briefly listed in Table 2.

Many of the methods listed here are GP models. GP models are useful as they adopt many properties inherent in the Gaussian normal distribution. Furthermore, the mathematical properties associated with the multivariate form allow matrix computations to be performed more efficiently for a small data set. A comprehensive elaboration on the GP in ML is written in this textbook [182]. Elaborated briefly, in the context of ML, the GP assumes the data points as a collection of random variables with joint Gaussian distributions with a mean value of zero. This then allows the covariance parameter to be tweaked as a smoothing parameter. The covariance between each distinct parameter is therefore reflected in the spatial distance between any two data points and is typically defined by a kernel function.

**Table 2. List of surrogate models using ML methods.**

Optimization method	AM technique	Material	Optimization problem and study	Ref.
ANN with Monte-Carlo simulation	EBM	CoCr	Optimal process map, porosity	[169]
RFN	PBF	IN718	Porosity	[178]
GP with metropolis-hastings MCMC algorithm	PBF	SS316L	Melt pool dimensions	[168]
GP model with Bayesian estimation	PBF	17-4PHSS	Porosity	[179]
GP with regression tree	SLM	SS316L	Melt pool dimensions	[180]
GP	PBF	SS316L and 17-4PHSS	Porosity	[181]
Deep learning with ANN	SLM	Ti6Al4V	Porosity	[177]
ANN	DED	Ti6Al4V	Porosity and build height	[176]

The advantage of the GP model is its relatively easy implementation and ability to smooth out noisy environments with a limited number of training data. This makes GP an “efficient and effective regression tool with few input features and a small data set” [172]. However, when the number of data increases or the size of the input increases, we can expect the performance of the GP to decrease as the computation for the inversion of a growing  $N \times N$  matrix will be increasingly expensive. Regardless, given a sufficiently large amount of data, the application of the GP is able to predict relatively accurate results. For example, a surrogate model obtained from a GP response surface fitted with 139 samples showed that the error of the prediction was within measurement error [168].

In contrast, neural networks (NNs) contain multiple hidden layers that connect an input and output layer. Similar to biological neural systems, every node in the hidden layers is connected to one another via an activation function. One then seeks to minimize the error of prediction by minimizing the associated weight for each connection, commonly through a back-propagation algorithm based on gradient descent. Even though no *a priori* relations were known between the input and output factors, the NN is able to “learn” the relations and predict outputs given certain combination of inputs, such as determining the optimal parameter set for the minimal porosity of SLM Ti6Al4V [177]. Although both the GP and NNs do not entirely describe the physics of AM, they can be used as surrogate models for both optimal processing window predictions and multi-objective optimization problems. The use of ML may help uncover some physical relations only with human interpretation.

Depending on the application, the choice of the surrogate model can be selected based on its unique advantages or limitations [183,184]. For example, An *et al.* showed that GP works well only when the covariance function is properly defined, while neural networks perform better for complex high-dimensional models with large noise, though huge amounts of training data sets are required [185]. Moreover, surrogate models can be chosen based on the data characteristics. For example, RSM is better able to approximate the overall trend of true models and performs well at fitting convex problems [186,187]. In contrast, Kriging, radial basis functions and support vector regression are more suitable for multi-modal and non-linear problems [187,188]. Within these functions, RBF is recommended for high-order non-linear problems, while Kriging is recommended for low-order nonlinear problem in high-dimensional space [183,189]. Therefore, the data characteristics determine the application of surrogate models. The same can be said for process parameter searching and optimization. As seen in articles utilizing the processing window approach, in most alloy systems, the porosity change due to power and velocity is relatively smooth. Thus, RSM has been the popular choice to describe such trends. However, when a greater number of parameters are considered, a higher dimensional data set is encountered. In these cases, the response has often been described as non-linear. Hence, ANN approaches are popular to describe multiple-input and multiple-output problems.

### Optimization: single- and multi-objective

#### *Overview of optimization algorithms*

There are two phases of optimization of the process parameters in AM. In the first phase, the optimal processing window is identified. The second phase is the application of multi-objective optimization algorithms within the

processing window, via an appropriate surrogate or mechanistic model of the PSP. Generally, this distinction can also be viewed as a “rough” and “fine” optimization, as it is more practical to first reduce the search in global space and subsequently optimize within a locally defined space.

In AM, commonly identified objectives include the minimization of build time, energy consumption, reducing porosity and improving mechanical properties. If a single-objective optimization problem is defined (such as porosity), there are straightforward algorithms that can obtain the minimum (or maximum) response value. However in AM, multiple conflicting objectives are often encountered. For example, build time has always been criticized as a main setback for the wide adoption of AM. Two main process parameters are physically relevant in influencing the build time, namely, the scanning speed and layer thickness. Although there is a great incentive to increase scanning speeds to minimize build time, reduce energy consumption and processing cost, the corresponding heat input power is effectively reduced which may lead to poor densification (Section 3). Higher scan speeds could also increase cooling rate, which can achieve finer grains and microstructures<sup>[190,191]</sup>, with a tradeoff in ductility. Hence, unless better microstructural features can be obtained for printing at lower speeds, processing at the highest scanning speed possible is always desired. In contrast, increasing the layer thickness reduces the number of layers for printing, thus decreasing the build time. Therefore, for the shortest possible build time, the greatest possible layer thickness should be adopted, provided that there is no compromise to part property due to defect formation. For example, Leicht *et al.* showed that in the SLM of stainless steel, increasing the layer thickness up to 80  $\mu\text{m}$  still yielded acceptable tensile properties<sup>[192]</sup>. Necessarily, the build height of the designed object directly influences the build time, which in turn is directly related to its build orientation, while surface roughness requirements will subsequently be affected depending on whether it is upskin or downskin.

Hence, AM usually presents itself as a multi-objective optimization problem and multi-objective optimization algorithms are required to narrow and refine the parameter space in AM, provided that the input-output relations are known. Much of the work in the previous decade has been on the processing window for AM and the literature for user-defined multi-objective optimization in metal-based AM is limited but growing. It is clear that the main obstacle for achieving full a priori multi-objective optimization capability in AM is the availability of accurate and reliable models for the optimization function. It is also possible that one can carry out multi-objective optimization studies in welding<sup>[193]</sup> or non-metal AM<sup>[194]</sup> and subsequently implement similar methodologies into metal AM.

The general multi-objective optimization problem (MOP) can be expressed as follows:

$$\begin{aligned} \min F(X) &= (f_1(X), f_2(X), \dots, f_r(X)) \quad X \in \Omega \in R^n \\ \text{s.t } g_i(X) &\leq 0 \quad i = 1, 2, \dots, k \end{aligned} \quad (1)$$

where  $f_i(X)$  ( $i = 1, 2, \dots, r$ ) is a sub-objective of the optimization problem,  $X = (x_1, x_2, \dots, x_n)$  is the decision vector,  $\Omega$  is the decision space and  $g_i(X) \leq 0$  ( $i = 1, 2, \dots, k$ ) is the constraint function. Multi-objective optimization methods can be divided into three categories based on their decision-making methods: pre-decision methods; post-decision methods; interactive decision-making methods<sup>[195]</sup>.

#### (1) Pre-decision methods

The pre-decision method (including scalarization approach<sup>[196]</sup>) gives decision information before optimizing the search and the weighted sum method is one of the most representative methods. The weighted sum method converts multi-objective optimization into a single-objective problem solving by assigning different weight values to sub-objectives<sup>[197]</sup>:

$$\begin{aligned} \min F(X) &= \sum_{i=1}^r \omega_i f_i(X) \quad X \in \Omega \in R^n \\ \text{s.t } g_i(X) &\leq 0 \quad i = 1, 2, \dots, k \end{aligned} \quad (2)$$

where  $\omega_i$  is the weight of the  $i^{th}$  sub-objective. The weighted sum method is the simplest and most direct method to solve multi-objective problems, but it is difficult to obtain the optimal solution for non-convex search spaces.

### (2) Post-decision methods

The post-decision method first generates a set of solutions that are optimal for some sub-objectives or that all sub-objectives are “non-inferior” for decision makers to choose. Non-dominated sorting is a typical representative of post-decision-making methods and it is also a widely used multi-objective solution method. The optimal solution of a multi-objective problem is a set of non-dominated solutions and the set of all non-dominated solutions constitutes a non-dominated solution set. If and only if  $X_1, X_2$  satisfy the following relationship:

$$\begin{aligned} \forall i \in \{1, 2, \dots, r\}, f_i(X_1) \leq f_i(X_2) \\ \wedge \exists i \in \{1, 2, \dots, r\}, f_i(X_1) < f_i(X_2) \end{aligned} \quad (3)$$

then  $X_1$  dominates  $X_2$ , expressed as  $X_1 > X_2$ . In addition, if and only if the following relationship is satisfied:

$$\{X \in \Omega \mid X > X_1\} = \emptyset \quad (4)$$

then there is no other feasible solution to dominate  $X_1$  in the decision space and  $X_1$  is deemed a non-dominated solution of  $\min F(X)$ .

### (3) Interactive decision-making methods

The interactive decision-making method is realized through the continuous interaction of the process of decision-making and optimization. In the optimization process, both pre- and post-decision methods may be used. For example, with variable weight optimization, the weight value of each sub-objective is adjusted in real time according to the results of the previous optimization. The interactive decision-making method is difficult to determine the decision preference in advance, so the efficiency of the optimization process is low.

Usually, there is no unique combination of the process parameter inputs that can maximize all response outputs. For any vector in the design space, the improvement in one of the objective functions may lead to the deterioration of another objective function. The low or negative correlation between any two objective functions does not guarantee a direct improvement in the result obtained when one of the objective functions has been improved. Therefore, a Pareto optimal solution is obtained, which describes a non-dominated solution on the objective space that represents a possible vector input given the compromises imposed by the conflicting objectives. Multiple Pareto optimal solutions can be obtained, and the set of Pareto optimal solutions is known as the Pareto front. A key goal in performing multi-objective optimization is to achieve an acceptable trade-off between conflicting objective responses within reasonable computation time. Although no absolute optimum is obtained, it is still necessary to explore the Pareto front to understand how outputs can be maximized given the existing trade-offs.

### *Application of multi-objective optimization algorithms*

The aforementioned optimization problems are now mostly solved with intelligent optimization algorithms, including evolutionary algorithms, which are stochastic approaches that mimic evolution theory and gene selection. Such algorithms are inspired by human intelligence, the social nature of biological groups and the laws of natural phenomena. The algorithm first generates a random population sample with genes assigned to different properties in the input. The “evolution” occurs by selecting favorable genes, i.e., inputs with correspondingly favorable outputs, and allowing both “crossover” and “mutation” to generate a new population with a new set of genes. The iteration process is halted when a favorable sample size is obtained. In fact, most multi-objective optimization studies in AM available in the literature use some form of evolutionary approach. However, these studies have mostly been demonstrative. [Table 3](#) summarizes these multi-objective optimization techniques, which includes non-dominated sorting genetic algorithms (NSGAs), multi-objective particle

**Table 3. Summary of methods used in multi-objective optimization for metal AM**

Optimization method	AM technique	Material	Study	Ref.
NSGA & MOPSO	SLS	General	Minimize surface roughness and time	[198]
MOGA	DMD	Ti-6Al-4V & Inconel 718	Powder waste & laser energy consumption	[199]
MOGA	SLS	General	surface roughness and energy consumption	[200]
NSGA-II	SLM	Ti6Al4V powders	weight and mechanical performance of the structure	[201]
m-APO	SLM	Ti6Al4V	Mechanical properties of material(modulus of elasticity and ultimate tensile strength)	[197]
NSGA	SLM	SS316L	Surface roughness, tensile strength and time consumption	[202]

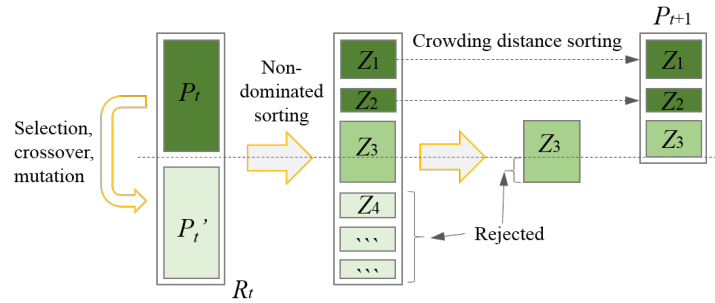


**Figure 7.** An iteration process of NSGA-II.

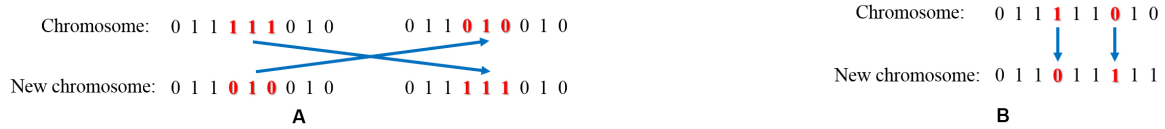


**Figure 8.** (A) Crossover and (B) mutation operators of NSGA-II, which changes the chromosomes in each iteration.

swarm optimization (MOPSO), multi-objective genetic algorithms (MOGAs) and multi-objective accelerated process optimization (m-APO). These methods differ in terms of their selection process for the optimal solution, as elaborated in the subsequent paragraphs.

The NSGA-II algorithm is famous for its elitist and fast computations<sup>[203]</sup> and is one of the most popular evolutionary algorithm for optimization in AM<sup>[198,204]</sup> and other processing communities. The criteria for selection of the optimal solution is determined by the Pareto dominance and crowding distance, and the obtained solution possesses elite preservation and explicit diversity preserving mechanisms, which ensure good convergence and diversity.

The main operations of NSGA-II include fitness calculations, non-dominated sorting, crowding distance evaluation, selection, crossover and mutation. [Figure 7](#) illustrates an iteration process of NSGA-II and its key operations<sup>[205]</sup>. During the  $t^{th}$  iteration of NSGA-II, it begins by choosing from the current population  $P_t$  and the solutions will go through crossover and mutation, as shown in [Figure 8](#). The new population  $P_t'$  is combined with  $P_t$  to construct  $R_t$ . Individuals of  $R_t$  will be then sorted into different fronts,  $Z_1, Z_2, \dots$ , and solutions from the same front are non-dominated to each other. The initial population of the next iteration  $P_{t+1}$  is formed by choosing the solution fronts sequentially. In the case of adding a front  $Z_i$  resulting in overpopulation, the individuals of  $Z_i$  are sorted based on the corresponding crowding distances and only individuals with larger crowding distances are chosen to form  $P_{t+1}$ . These steps will be repeated until the exit criteria are met.

Padhye and Deb<sup>[198]</sup> used NSGA-II for multi-objective optimization in selective laser sintering, where surface roughness and build time were considered as the main objective functions. Furthermore, the implementation of performance measurements, such as attainment surface and hypervolume indicator, approximated the best non-dominated set from the available solutions and measured the diversity, as well as the convergence of the solutions. This result shows that the NSGA-II ensures good convergence and diversity. The use of decision choice is known as the “knee point”. Meng *et al.* used NSGA-II to solve a multi-objective optimization problem by formulating mathematical equations to represent the energy absorption and density of bio-inspired structures<sup>[201]</sup>. The most satisfactory Pareto points selected to be the solution are obtained by the use of the “knee point”, from the Pareto set. Meng *et al.* concluded that the NSGA-II can be used to optimize the mechanical properties of the fabricated product by SLM<sup>[201]</sup>. The experimental results obtained are larger than the optimization results due to the existence of manufacturing errors in the structural dimensions during SLM. The results obtained are slightly higher than the optimization result. However, the relative errors of all parameters are less than 10%, which shows that the multi-objective optimization model has a high predictive ability.

MOPSO is different in terms of the selection process for optimal solution, with the main difference of identifying the personal best (p-best) and global best (g-best)<sup>[206,207]</sup>. The use of MOPSO provides a reduction in computation time and improves the convergence performance of the solution. The obtained solutions have good convergence and a diversity and spread along the Pareto-optimal front. There are different strategies for selecting p-best and g-best, with random-random and dominance based probability strategies being the best performers. The potential solutions move through the search space, the solutions are known as particles and are associated with the position and velocity vectors<sup>[198]</sup>. The best position attained by the particle are attracted to the best of the particle attractors in a certain neighborhood. The method even includes a “turbulence factor” to preserve the diversity of the population and the searching process is made efficient by archiving the most recent non-dominated solutions<sup>[198]</sup>. Zhang *et al.* reported that this method was highly competitive in terms of convergence and diversity in comparison with other state-of-the-art algorithms<sup>[208]</sup>. This method can be applied to wide applications and the Pareto points from the result were the best possible solution. This method is capable of minimizing objectives simultaneously to obtain a set of non-dominated solutions. Padhye and Deb<sup>[198]</sup> explained the methodology and also showed that the major difference between MOPSO and PSO is the implementation of p-best and g-best. This result shows that the MOPSO encounters difficulties to optimize due to the absence of potential global guides and discontinuous function landscapes. Furthermore, the article also made a comparison between the obtained result to show that NSGA dominates MOPSO. There is a clear indication that MOPSO suffers from well-known drawback of premature convergence. The result also shows that NSGA outperforms MOPSO in most cases, by achieving better convergence and spread. Even though the majority of NSGA solutions dominate the MOPSO solutions, MOPSO is capable of finding better extreme solutions. While MOPSO provides a reduced computation cost, the cause was due to pre-mature convergence. This comparison clearly shows the superiority of NSGA and MOPSO.

The m-APO starts with a classical approach to the multi-objective problem. However, it differs from other methods in its space-filling methodology<sup>[151]</sup>. The space-filling method uses an analogy of electrical charges for the design points, where a higher magnitude of charges is assigned to a lower response value and that the design points would repel each other to obtain well-distributed Pareto points. This ensures a better diversity of solution among the mentioned optimization methods. Aboutaleb *et al.* applied this method onto a case study to identify optimal process parameters, which helps to optimize the mechanical properties of the end products<sup>[197]</sup>. The research gap identified by the researcher is the optimization of multiple mechanical properties of the fabricated part in an efficient manner. This method is able to effectively approximate the Pareto front with a few rounds of experiments by identifying and leveraging the similarities of the different sub-problems, which shortens the multi-objective optimization procedure. Aboutaleb *et al.* found that the computation cost for the optimization process using m-APO was reduced by 51.8%, as compared to the same Pareto solutions obtained from the extended full factorial design<sup>[151]</sup>. Aboutaleb *et al.* performed another study on this optimization

method and the result obtained also shows a reduction in the number of experiments by 20% as compared to a full factorial DOE plan<sup>[209]</sup>. This method is capable of providing the benefit of reduced computational cost for identifying the optimal solution as compared to a full factorial DOE plan.

MOGA is designed for fast Pareto convergence and was selected by Yan *et al.* to perform the optimization, where the energy cost and powder waste were viewed as two objective functions<sup>[199]</sup>. The result shows that the design greatly reduces the laser energy cost while mentioning that the real-time optimization is time consuming (several hours). Strano *et al.* also showed that using the MOGA for multi-objective optimization minimizes the surface roughness value by up to 50%<sup>[200]</sup>. The significant improvement in the result displayed the capability of MOGA method in finding solutions to find the required objective.

Although we acknowledge that these algorithms have different advantages and performance in terms of their convergence speed, spreadability of Pareto front and robustness (ability to reach global optima), we believe they are relatively insignificant at the current stage of process parameter optimization for AM research. The minute differences in computational speed required between the optimization algorithms are inconsequential compared to the modelling efforts and computational requirements for parameter search via mechanistic or data-driven models. Moreover, studies with RSM and SVM have shown that the output responses of current parameters of interest (e.g., porosity) are relatively smooth. Hence, the performance of these optimization algorithms applied in current scenarios are likely to be similar. Therefore, the choice of multi-objective optimization algorithm has hitherto less significance. Nonetheless, they are listed for completeness to illustrate the approaches used in AM research. NGS-II can be recommended as it is a popular and relatively easy algorithm to apply and is included in most software packages.

## DISCUSSION

The discussion of the various techniques in DoE, data collection and modelling is tabulated in [Table 4](#). However, comparisons between optimization algorithms have been left out as we believe it should not be the main focus for current research in process parameter optimization of AM.

Despite the different techniques offered to evaluate optimal process parameters for manufacturing, we believe that the straightforward full-factorial design experimental work will remain as the primary method as it is direct and reliable. This is pertinently true for the development of process parameters for new alloys with unknown behavior or novel processing techniques with unknown mechanisms. Statistical methods may not provide the same level of resolution for unexplored parameter space and the presupposition that the system behavior is well behaved outside the scope of study may not be true. However, when finding parameters for well-known alloys (e.g., SS316L, Ti-6Al-4V and IN625) in a new system (i.e., a new machine or powder obtained from a different supplier), statistical methods are recommended because previous studies have already demonstrated that the output responses of the entire processing map are relatively smooth (mild gradient changes).

While it is one of the goals for mechanistic numerical models to replace the number of experiments for parameter searching, we believe that current simulations models remain relatively immature for comprehensive behavioral predictions of new alloy systems. More work is needed to evaluate the thermodynamic behavior between elements and their environment during AM processing. Thus, experimental techniques for parameter finding remain necessary. Nonetheless, validated simulations for known alloys can be used to assist in parametric studies under new systems (i.e., a new machine), though to a limited extent. Many parameters in current simulations are empirical yet crucial for numerical results, e.g., heat transfer coefficients, fluid flow coefficients and so on, which are heavily dependent on system characteristics. Overall, more work is needed in simulations to provide a sufficient level of capability to predict or at least guide the search for process parameters for new

**Table 4. Summary of the methodologies, their advantages, disadvantages and their applicability in AM**

Methodology	Advantages	Disadvantages	Applicability in process parameter search and optimization
<b>Design of Experiments (Data sampling strategy)</b>			
Full factorial design	<ul style="list-style-type: none"> <li>Simple and straightforward</li> <li>Able to capture interaction effects to a limited degree</li> <li>Allows application of RSM to approximately quantify changes</li> </ul>	<ul style="list-style-type: none"> <li>Number of experiments or samples needed grows exponentially when number of levels and factors analyzed increases</li> </ul>	The most common and straightforward method due to ease of application with no expertise required. Direct analysis can be performed whenever results are obtained. Without comprehensive models, full factorial design is still recommended for investigations into new alloys, novel methods or techniques.
Taguchi (and fractional) factorial designs	<ul style="list-style-type: none"> <li>Orthogonality significantly reduces the number of experiments required</li> <li>Allows consideration of more parameters</li> <li>Allows identification of key parameters</li> </ul>	<ul style="list-style-type: none"> <li>Requires some level of experience to determine control and noise variables</li> <li>Does not show interaction effects</li> </ul>	Taguchi's method is inherently more effective for early stage of AM process search. As we have now some level of understanding of key process parameters, the effectiveness of Taguchi method has waned. Nonetheless, it can still be used for exploration of unstudied parameters, but they will not be comprehensive.
<b>Characterization (Data collection)</b>			
Experiments	<ul style="list-style-type: none"> <li>Ground truth</li> <li>Relatively straightforward process</li> </ul>	<ul style="list-style-type: none"> <li>Characterization process is time consuming and resource intensive</li> </ul>	Although time consuming, experiments are still the ground-truth, needed for validation. In process parameter search, statistical methods are recommended for alloys with previous studies that show relatively linear responses.
Surrogate models for data generation	<ul style="list-style-type: none"> <li>Computationally inexpensive for sufficiently accurate results</li> </ul>	<ul style="list-style-type: none"> <li>Reliability of model heavily depends on accuracy of the data</li> </ul>	Probably the most practical option for process parameter search via simulation. Highly recommended for future multi-objective optimization studies.
<b>Modelling</b>			
Analytical mechanistic models	<ul style="list-style-type: none"> <li>Almost-instantaneous calculation</li> </ul>	<ul style="list-style-type: none"> <li>Mostly valid for conduction-mode regimes</li> </ul>	Only for approximating melt pool dimensions and temperature field. Analytical models have frequently been used for outlining the process parameter space, but it is usually inaccurate and requires further calibration.
High-fidelity numerical mechanistic models	<ul style="list-style-type: none"> <li>Considers complex multi-physics interactions</li> <li>High-fidelity and interpretable results</li> </ul>	<ul style="list-style-type: none"> <li>Computationally expensive</li> <li>Mostly proprietary codes</li> </ul>	Validated models have been developed but remain lacking in accounting physical phenomena. With sufficient level of fidelity, these models should be used for the behaviour prediction of new alloys systems and processing conditions. Results from these models should be converted into surrogate models for multi-objective optimization studies.
Regression (Linear or multi-dimensional)	<ul style="list-style-type: none"> <li>Straightforward</li> <li>Easy to implement</li> </ul>	<ul style="list-style-type: none"> <li>Limited and simplified analysis</li> <li>Interaction effects may not be captured</li> </ul>	Frequently used to quantify output responses with VED, though with limited success as studies have shown that some input parameters have greater effects. Recommended only for early exploration and simple quantification, and for non-dimensionalization methods.
Response surface methodology	<ul style="list-style-type: none"> <li>Straightforward and easy to visualize</li> <li>Relatively accurate for convex responses</li> </ul>	<ul style="list-style-type: none"> <li>Mostly applicable for 3 variables</li> <li>Performs better only when response surface is smooth</li> <li>Higher dimensional surfaces</li> </ul>	Frequently used with full factorial studies to describe the output response of the study. May be sufficient for industry use and multi-objective optimization study, if the target output responses behave smoothly.
Surface vector machines	<ul style="list-style-type: none"> <li>Suitable for classification (or regression) of high-dimensional data</li> </ul>	<ul style="list-style-type: none"> <li>Requires appropriate kernel function</li> <li>Limited interpretability</li> </ul>	SVM has been used for in-situ monitoring (classification of defects), classification of melting modes and outlining in process maps. Recommended for in-situ monitoring and optimization applications.
Gaussian Process	<ul style="list-style-type: none"> <li>Easy to implement</li> <li>Smooths out noisy data</li> </ul>	<ul style="list-style-type: none"> <li>Suffers when covariance matrix is ill-defined</li> </ul>	Recommended for surrogate modelling when experimental datasets are available and uncertainty quantification.

alloys and systems.

On the topic of modelling, mechanistic (physics-based) and surrogate (data-driven) models are often compared with the main contrasts in their computational requirements and the interpretability of the results.

Kouraytem *et al.* provided a comprehensive discussion and comparison between physics-based and data-driven models used in AM<sup>[162]</sup>. For parameter searching in process parameter optimization, computational speed and accuracy are key<sup>[147,167]</sup>. Thus, surrogate models are more practical for searching the parameter space due to their significantly reduced computational requirements. Interpretability is not a significant issue in this regard. The prediction speed offered by surrogate models can even allow the possibility of real-time in-situ monitoring and optimization. Regardless, the generation of surrogate models does not preclude the need for data acquisition and collection. To generate such data via experiments, considerable lead time will be incurred. Therefore, validated mechanistic models can replace experiment work for the generation of data points. Subsequently, surrogate models can be developed with reference to these generated points for process parameter searching.

While different techniques can be used in metal AM, their optimization frameworks are similar. The approaches for DoE, characterization, modelling and optimization algorithms do not have specific advantages when applied in any metal AM technique. However, the prioritization of the objectives during optimization may differ due to differences in the processing mechanism. For example, Mukherjee and Debroy<sup>[210]</sup> compared the printability of SS316L via PBF, DED with a laser and DED with a gas metal arc heat source. They found that the percentage changes in the output responses (residual stress, distortion and chemical composition) are different based on techniques, i.e., chemical composition changes are larger for PBF but residual stresses and distortion issues are more crucial for DED. Hence, the optimal process parameters for PBF can be more influenced towards reducing the changes in chemical composition, while the optimal process parameters for DED are more oriented towards reducing distortion. Similarly, with the AM of copper<sup>[211]</sup> as an example, we observe that tuning the optical absorptivity and atmosphere control has a larger influence on processing copper for laser-based processes; however, these are not problems in electron-beam processes. Therefore, process parameters for laser-based processes are selected near the stable keyhole mode to achieve better bonding. Hence, the prioritization of objectives for optimization studies will likely be different for different AM methods. If densification is the primary objective, the AM practitioner must thereafter prioritize the objectives for optimization based on the AM technique and application requirements.

It should be reiterated that in AM optimization, there is no one-size-fits-all rule for the determination of design objectives and constraints. The determination of which output parameters are objectives and constraints is wholly context dependent. For example, while it is common to desire zero-porosity parts with low surface roughness for engineering applications due to fatigue considerations, high porosity and surface roughness are actually desirable characteristics in the AM part for bone grafts in biomedical applications for osseointegration<sup>[131]</sup>.

## CONCLUSION

### Research gaps

There are two aspects to consider when considering the research gaps of process parameter optimization. The first pertains to gaps for process parameter searching, while the second pertains to factors that limit the possibility of multi-objective optimization studies. Collectively, the key gaps we found for process parameter searching are (i) the incomplete understanding and awareness of process parameters, (ii) the difficulty in understanding the chemical changes during processing and (iii) a lack of reliable high-throughput models with rapid computational times.

The multi-objective optimization problem is a hugely relevant problem for industrial applications but is under-researched as it is hindered by a key issue, i.e., a lack of accurate PSP models with reasonable computation time. While optimal processing windows have been obtained for many materials, there are no universal models to describe response outputs due to the inputs. Although this gap is partly filled by the development of

numerical models, the direct application of these models into optimization problems is computationally unfeasible. In fact, current numerical models remain lacking. For example, with present knowledge and capabilities, the reliable and comprehensive prediction of microstructures for new alloys remains unattainable. Microstructural research in AM remains an intrinsically material-specific problem and requires characterization studies, especially where alloying physics under intense evaporation, huge compositional inhomogeneity and unprecedented cooling rates remain largely unknown. More research is needed to develop the material and thermodynamic database and computational tools to predict the microstructures at different process parameter combinations. As numerical models become increasingly complex, there will be the a need to convert the high-fidelity but time-consuming models into appropriate surrogate models for efficient computation. Furthermore, although impressive high-fidelity models have been developed for AM at different length scales, the linkage between these different scales remains lacking, e.g., how to reliably estimate the bulk thermal history of multi-layers and multi-tracks based on the high-fidelity simulations of a single track. As experimental and numerical data for metal AM increases, ML will definitely play a role in shaping AM research. However, a pure black-box model approach commonly used in ML, while feasible, would not be sufficient for a thorough understanding of the underlying physics. Instead, a hybrid physics-based ML for metal AM may be a better approach to incorporate both well-known physics and unknown correlations in AM<sup>[212,213]</sup>. We believe that higher resolution imaging techniques will continue to be relevant for the experimental validation of numerical models to better understand the rapid melting and solidification of the AM process.

Moreover, the comparison of results between published studies remains highly limited. Firstly, the use of different materials prohibits direct comparison, especially due to different characteristic crystallographic textures. Nonetheless, the use of normalized diagrams or non-dimensional variables<sup>[115,116]</sup>, subjected to introduction of physically motivated tweaking parameters, may be able to address the non-comparability between different materials. A dimensionless parameter that is consistent for comparison may suggest universality in metal AM regardless of the material applied. Secondly, the comparison of data is difficult when the metal AM process is sensitive to variances in equipment and powder used in metal AM, leading to reproducibility issues even within the same powders or equipment. The issue of reliability and reproducibility reiterates the problem of standardization, which remains due to lack of understanding, or even awareness, of factors that can affect the AM process. As characterization of AM parts of the same material yield different results, quantification and standardization becomes difficult. A key problem which remains under-researched, is the chemical compositional differences that arise during processing. Minute changes in chemical compositions of alloys can affect the thermodynamic behavior of the phase system, and thus, their properties. The difficulty is compounded as the physio-chemical behavior of the alloys under intense evaporation and cooling rates make in-depth, in-situ experimental investigations nigh impossible. Moreover, AM machines have many components (laser, piston, sensors, spreader, actuators, motors and so on) and their wear and tear may influence the factors that affect heat input and chemical variations. Uncertainty and variation remain key issues in AM, which deserves another review altogether.

For future optimization problems, especially for the identification of processing regions for new alloys, an increasing refining approach is recommended. By using already existing scaling laws and non-dimensional models, an initial processing region can be first estimated. Data can be sampled within an initial processing space either with experiments or simulations. Surrogate models can therefore be developed in two aspects, namely, surrogate models for simulations or surrogate models for the entire process space. The entire goal is to reduce the computational resource and experimental effort required to evaluate the process space such that the 'optimal' parameter can be found.

### **Future outlook**

At the core of many scientific questions in metal AM is the materials science of metal AM, which has a characteristic high thermal gradient and rapid solidification at the microscale during manufacturing, leading to the

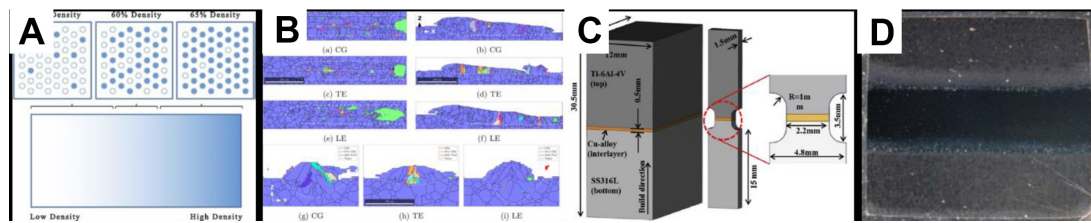


**Figure 9.** Tailored microstructures and materials using additive manufacturing: (A) functionally graded density [214]; (B) tailored microstructures via beam shaping [215]; (C) AM of Ti6Al4V bonded with SS316L with copper acting as intermediary [216]; (D) AM of CuCrZr with Steel 1.2790 [217].

formation of microstructural patterns and textures not achievable or encountered in traditional metallurgy. This requires current research to update current knowledge in AM-focused metallurgy. As such, PSP relations remain a central focus for AM research.

However, for the AM practitioner for industrial and application purposes, applied methods would be of greater interest. In the big picture, process parameter optimization is only a small but crucial part in the process chain of metal AM. As such, models with sufficient accuracy and acceptable prediction capabilities are adequate for industrial needs. As much of optimization work in AM is largely empirical and statistical, there will be an increasing use of data-driven techniques and ML as tools for surrogate modelling and optimization. For application of ML in AM, we would expect a hybrid physics-based ML to be developed to combine physical knowledge while including uncaptured phenomena to optimize process parameters in design for AM. Surrogate models developed with high-fidelity simulations as the foundation are expected to help accelerate this field.

The precise control of process parameters theoretically allows the AM practitioner to fabricate parts down to the microscale, i.e., total microstructural control. This opens a myriad of design possibilities, such as functionally graded materials [214], tailored microstructures [215] and even multi-metal print capability [216,217], allowing creation of parts that are impossible in conventional manufacturing methods [Figure 9]. The realization of this exciting prospect (total microstructure control) in metal AM starts with having a strong foundation of optimization control and capability of the process parameters. With such possibilities, it is necessary for us to reflect and reconsider the notion of ‘optimal processing region’ merely from a densification perspective.

## DECLARATIONS

### Acknowledgments

The authors acknowledge members of the Yan Group for fruitful discussions towards the preparation of this work.

### Authors' contributions

Proposed and conceived the review, collated, analyzed and organized the literature, wrote and provided stylistic/grammatical revision on the manuscript: Chia HY

Collated, analyzed and organized the literature, wrote and provided stylistic/grammatical revision on the manuscript: Wu J, Wang X

Provided supervision, acquired funding, wrote and provided stylistic/grammatical revision on the manuscript: Yan W

### Availability of data and materials

Not applicable.

### Financial support and sponsorship

This research is supported by the Ministry of Education, Singapore, under its Academic Research Fund Tier 2 (MOE-T2EP50121-0017). Financial support from the Presidential Graduate Fellowship at the National University of Singapore is gratefully acknowledged by Hou Yi Chia.

### Conflicts of interest

All authors declared that there are no conflicts of interest.

### Ethical approval and consent to participate

Not applicable.

### Consent for publication

Not applicable.

### Copyright

© The Author(s) 2022.

## REFERENCES

1. Seifi M, Gorelik M, Waller J, et al. Progress towards metal additive manufacturing standardization to support qualification and certification. *JOM* 2017;69:439–55. DOI
2. AMSC. Standardization roadmap for additive manufacturing, version 2.0; 2018. Available from: [https://63.241.103.54/Shared%20Documents/%20Activities/AMSC/AMSC\\_Roadmap\\_June\\_2018.pdf](https://63.241.103.54/Shared%20Documents/%20Activities/AMSC/AMSC_Roadmap_June_2018.pdf) [Last accessed on 23 Sep 2022]. Available from: [https://share.ansi.org/SharedDocuments/StandardsActivities/AMSC/AMSC\\_Roadmap\\_June\\_2018.pdf](https://share.ansi.org/SharedDocuments/StandardsActivities/AMSC/AMSC_Roadmap_June_2018.pdf).
3. AMSC. April 2022 Progress Report on AMSC Roadmap v2 Gaps; 2022. Available from: [https://share.ansi.org/SharedDocuments/StandardsActivities/AMSC/April\\_2022\\_Progress\\_Report\\_AMSC\\_Roadmap\\_v2\\_Gaps.pdf](https://share.ansi.org/SharedDocuments/StandardsActivities/AMSC/April_2022_Progress_Report_AMSC_Roadmap_v2_Gaps.pdf) [Last accessed on 23 Sep 2022].
4. Additive manufacturing-design-requirements, guidelines and recommendations. Geneva, CH: International Organization for Standardization; 2018. DOI
5. Gu DD, Meiners W, Wissenbach K, Poprawe R. Laser additive manufacturing of metallic components: materials, processes and mechanisms. *Int Mater Rev* 2012;57:133–64. DOI
6. Yap CY, Chua CK, Dong ZL, et al. Review of selective laser melting: materials and applications. *Appl Phys Rev* 2015;2:041101. DOI
7. Svetlizky D, Das M, Zheng B, et al. Directed energy deposition (DED) additive manufacturing: Physical characteristics, defects, challenges and applications. *Mater Today* 2021;49:271–95. DOI
8. Cunningham RW. Defect formation mechanisms in powder-bed metal additive manufacturing. Carnegie Mellon University; 2018. DOI
9. Kim FH, Kim FH, Moylan SP. Literature review of metal additive manufacturing defects. US Department of Commerce, National Institute of Standards and Technology; 2018. DOI
10. Brennan M, Keist J, Palmer T. Defects in metal additive manufacturing processes. *J Mater Engin Perform* 2021:1–11. DOI
11. Carter LN, Wang X, Read N, et al. Process optimisation of selective laser melting using energy density model for nickel based superalloys. *Mater Sci Techn* 2016;32:657–61. DOI
12. Fayazfar H, Salarian M, Rogalsky A, et al. A critical review of powder-based additive manufacturing of ferrous alloys: process parameters, microstructure and mechanical properties. *Mater Des* 2018;144:98–128. DOI
13. Liu S, Shin YC. Additive manufacturing of Ti6Al4V alloy: A review. *Mater Des* 2019;164:107552. DOI
14. Gong H, Rafi K, Gu H, et al. Influence of defects on mechanical properties of Ti–6Al–4 V components produced by selective laser melting and electron beam melting. *Mater Des* 2015;86:545–54. DOI
15. Du Plessis A, Yadroitsava I, Yadroitsev I. Effects of defects on mechanical properties in metal additive manufacturing: A review focusing on X-ray tomography insights. *Mater Des* 2020;187:108385. DOI
16. Kasperovich G, Haubrich J, Gussone J, Requena G. Correlation between porosity and processing parameters in TiAl6V4 produced by selective laser melting. *Mater Des* 2016;105:160–70. DOI
17. Snow Z, Nassar A, Reutzel EW. Review of the formation and impact of flaws in powder bed fusion additive manufacturing. *Addit Manuf* 2020:101457. DOI
18. Li C, Liu Z, Fang X, Guo Y. Residual stress in metal additive manufacturing. *Proced Cirp* 2018;71:348–53. DOI
19. Mercelis P, Kruth JP. Residual stresses in selective laser sintering and selective laser melting. *Rapid Prototyping J* 2006;12:254–65. DOI
20. Denlinger ER, Heigel JC, Michaleris P. Residual stress and distortion modeling of electron beam direct manufacturing Ti-6Al-4V. *Proc Instit Mechan Engin, Part B: J Engin Manuf* 2015;229:1803–13. DOI
21. Harrison NJ, Todd I, Mumtaz K. Reduction of micro-cracking in nickel superalloys processed by selective laser melting: a fundamental alloy design approach. *Act Material* 2015;94:59–68. DOI
22. Bauereiß A, Scharowsky T, Körner C. Defect generation and propagation mechanism during additive manufacturing by selective beam

- melting. *J Mater Proc Techn* 2014;214:2522–8. DOI
23. Chen F, Yan W. High-fidelity modelling of thermal stress for additive manufacturing by linking thermal-fluid and mechanical models. *Mater Des* 2020;196:109185. DOI
  24. Mukherjee T, Zhang W, DebRoy T. An improved prediction of residual stresses and distortion in additive manufacturing. *Comput Mater Sci* 2017;126:360–72. DOI
  25. Liang X, Chen Q, Cheng L, Hayduke D, To AC. Modified inherent strain method for efficient prediction of residual deformation in direct metal laser sintered components. *Comput Mech* 2019;64:1719–33. DOI
  26. Prabhakar P, Sames WJ, Dehoff R, Babu SS. Computational modeling of residual stress formation during the electron beam melting process for Inconel 718. *Addit Manuf* 2015;7:83–91. DOI
  27. Bartlett JL, Li X. An overview of residual stresses in metal powder bed fusion. *Addit Manuf* 2019;27:131–49. DOI
  28. Shiomi M, Osakada K, Nakamura K, Yamashita T, Abe F. Residual stress within metallic model made by selective laser melting process. *CIRP ann* 2004;53:195–8. DOI
  29. Kruth JP, Froyen L, Van Vaerenbergh J, et al. Selective laser melting of iron-based powder. *J mater proc techn* 2004;149:616–22. DOI
  30. Vrancken B, Buls S, Kruth JP, Van Humbeeck J. Influence of preheating and oxygen content on selective laser melting of Ti6Al4V. In: Proceedings of the 16th RAPDASA Conference; 2015. Available from: <https://lirias.kuleuven.be/1748568?limo=0> [Last accessed on 23 Sep 2022].
  31. Roberts IA. *Investigation of residual stresses in the laser melting of metal powders in additive layer manufacturing* 2012. Available from: <https://wlv.openrepository.com/handle/2436/254913> [Last accessed on 23 Sep 2022]. Available from: <https://wlv.openrepository.com/handle/2436/254913>.
  32. Ali H, Ma L, Ghadbeigi H, Mumtaz K. In-situ residual stress reduction, martensitic decomposition and mechanical properties enhancement through high temperature powder bed pre-heating of selective laser melted Ti6Al4V. *Mater Sci Engin: A* 2017;695:211–20. DOI
  33. Corbin DJ, Nassar AR, Reutzler EW, Beese AM, Michaleris P. Effect of Substrate thickness and preheating on the distortion of laser deposited Ti–6Al–4V. *J Manuf Sci Engin* 2018;140. DOI
  34. Calta NP, Martin AA, Hammons JA, et al. Pressure dependence of the laser-metal interaction under laser powder bed fusion conditions probed by in situ X-ray imaging. *Addit Manuf* 2020;32:101084. DOI
  35. Wang L, Zhang Y, Chia HY, Yan W. Mechanism of keyhole pore formation in metal additive manufacturing. *npj Comput Mater* 2022;8:1–11. DOI
  36. Yan F, Xiong W, Faierson E, Olson GB. Characterization of nano-scale oxides in austenitic stainless steel processed by powder bed fusion. *Script Mater* 2018;155:104–8. DOI
  37. Haines MP, Peter NJ, Babu S, Jäggle EA. In-situ synthesis of oxides by reactive process atmospheres during L-PBF of stainless steel. *Addit Manuf* 2020;33:101178. DOI
  38. Ikehata H, Mayweg D, Jäggle E. Grain refinement of Fe–Ti alloys fabricated by laser powder bed fusion. *Mater Des* 2021;204:109665. DOI
  39. Shen H, Rometsch P, Wu X, Huang A. Influence of gas flow speed on laser plume attenuation and powder bed particle pickup in laser powder bed fusion. *JoM* 2020;72:1039–51. DOI
  40. Weaver J, Schlenoff A, Deisenroth D, et al. *Inert gas flow speed measurements in laser powder bed fusion additive manufacturing* 2021. DOI
  41. Caballero A, Suder W, Chen X, Pardal G, Williams S. Effect of shielding conditions on bead profile and melting behaviour in laser powder bed fusion additive manufacturing. *Addit Manuf* 2020;34:101342. DOI
  42. Reijonen J, Revuelta A, Riipinen T, Ruusuuvuori K, Puukko P. On the effect of shielding gas flow on porosity and melt pool geometry in laser powder bed fusion additive manufacturing. *Addit Manuf* 2020;32:101030. DOI
  43. Bidare P, Bitharas I, Ward R, Attallah M, Moore AJ. Fluid and particle dynamics in laser powder bed fusion. *Acta Materi* 2018;142:107–20. DOI
  44. Chen H, Yan W. Spattering and denudation in laser powder bed fusion process: multiphase flow modelling. *Acta Material* 2020;196:154–67. DOI
  45. Eo DR, Chung SG, Jeon JM, Cho JW. Melt pool oxidation and reduction in powder bed fusion. *Addit Manuf* 2021;41:101982. DOI
  46. Metelkova J, Kinds Y, Kempen K, et al. On the influence of laser defocusing in selective laser melting of 316L. *Addit Manuf* 2018;23:161–9. DOI
  47. Sow M, De Terris T, Castelnaou O, et al. Influence of beam diameter on Laser Powder Bed Fusion (L-PBF) process. *Addit Manuf* 2020;36:101532. DOI
  48. Ladewig A, Schlick G, Fisser M, Schulze V, Glatzel U. Influence of the shielding gas flow on the removal of process by-products in the selective laser melting process. *Addit Manuf* 2016;10:1–9. DOI
  49. Anwar AB, Pham QC. Study of the spatter distribution on the powder bed during selective laser melting. *Addit Manuf* 2018;22:86–97. DOI
  50. Martin JH, Yahata BD, Hundley JM, et al. 3D printing of high-strength aluminium alloys. *Nature* 2017;549:365–69. DOI
  51. Yang Z, Wang S, Zhu L, et al. Manipulating molten pool dynamics during metal 3D printing by ultrasound. *Appl Phys Rev* 2022;9:021416. DOI
  52. AlMangour B, Baek MS, Grzesiak D, Lee KA. Strengthening of stainless steel by titanium carbide addition and grain refinement during selective laser melting. *Mater Sci Engin: A* 2018;712:812–8. DOI
  53. Ghayoor M, Mirzababaei S, Lee K, et al. Strengthening of 304L stainless steel by addition of yttrium oxide and grain refinement during

- selective laser melting. In: 2019 International Solid Freeform Fabrication Symposium. University of Texas at Austin; 2019. DOI
54. Lin TC, Cao C, Sokoluk M, et al. Aluminum with dispersed nanoparticles by laser additive manufacturing. *Nature Comm* 2019;10:1–9. DOI
  55. Gao C, Wang Z, Xiao Z, et al. Selective laser melting of TiN nanoparticle-reinforced AlSi10Mg composite: microstructural, interfacial, and mechanical properties. *J Mater Proc Techn* 2020;281:116618. DOI
  56. Liu X, Liu Y, Zhou Z, et al. Grain refinement and crack inhibition of selective laser melted AA2024 aluminum alloy via inoculation with TiC–TiH<sub>2</sub>. *Mater Sci Engin: A* 2021;813:141171. DOI
  57. Zhai W, Zhou W, Nai SML. Grain refinement and strengthening of 316L stainless steel through addition of TiC nanoparticles and selective laser melting. *Mater Sci Engin: A* 2022;832:142460. DOI
  58. Xiao F, Wang S, Wang Y, et al. Niobium nanoparticle-enabled grain refinement of a crack-free high strength Al–Zn–Mg–Cu alloy manufactured by selective laser melting. *J Alloys Compo* 2022;900:163427. DOI
  59. Basariya MR, Srivastava V, Mukhopadhyay N. Microstructural characteristics and mechanical properties of carbon nanotube reinforced aluminum alloy composites produced by ball milling. *Mater Des* 2014;64:542–9. DOI
  60. Wang P, Zhang B, Tan CC, et al. Microstructural characteristics and mechanical properties of carbon nanotube reinforced Inconel 625 parts fabricated by selective laser melting. *Mater Sci Techn* 2016;112:290–9. DOI
  61. Wang LZ, Chen T, Wang S. Microstructural characteristics and mechanical properties of carbon nanotube reinforced AlSi10Mg composites fabricated by selective laser melting. *Optik* 2017;143:173–9. DOI
  62. Kao A, Gan T, Tonyr C, Krastins I, Pericleous K. Thermolectric magnetohydrodynamic control of melt pool dynamics and microstructure evolution in additive manufacturing. *Phil Trans Royal Soci A* 2020;378:20190249. DOI
  63. Wang L, Yan W. Thermolectric magnetohydrodynamic model for laser-based metal additive manufacturing. *Phys Rev Appl* 2021;15:064051. DOI
  64. Lores A, Azurmendi N, Agote I, Zuza E. A review on recent developments in binder jetting metal additive manufacturing: materials and process characteristics. *Powd Metall* 2019;62:267–96. DOI
  65. Ziaee M, Crane NB. Binder jetting: a review of process, materials, and methods. *Addit Manuf* 2019;28:781–801. DOI
  66. Li M, Du W, Elwany A, Pei Z, Ma C. Metal binder jetting additive manufacturing: a literature review. *J Manuf Sci Engin* 2020;142. DOI
  67. Sun S, Brandt M, Easton M. Powder bed fusion processes: an overview. *Laser addit manuf* 2017:55–77. DOI
  68. Escano LI, Parab ND, Xiong L, et al. Revealing particle-scale powder spreading dynamics in powder-bed-based additive manufacturing process by high-speed x-ray imaging. *Sci rep* 2018;8:1–11. DOI
  69. Zhao C, Parab ND, Li X, et al. Critical instability at moving keyhole tip generates porosity in laser melting. *Science* 2020;370:1080–86. DOI
  70. Bitharas I, Parab N, Zhao C, et al. The interplay between vapour, liquid, and solid phases in laser powder bed fusion. *Nat Comm* 2022;13:1–12. DOI
  71. Sola A, Nouri A. Microstructural porosity in additive manufacturing: The formation and detection of pores in metal parts fabricated by powder bed fusion. *J Adv Manuf Proc* 2019;1:e10021. DOI
  72. Levkulich NC. An experimental investigation of residual stress development during selective laser melting of Ti-6Al-4V. Wright State University; 2017. Available from: [https://etd.ohiolink.edu/apexprod/rws\\_olink/r/1501/10?clear=10&p10\\_accession\\_num=wright1515112797193544](https://etd.ohiolink.edu/apexprod/rws_olink/r/1501/10?clear=10&p10_accession_num=wright1515112797193544) [Last accessed on 23 Sep 2022].
  73. Chen Q, Liang X, Hayduke D, et al. An inherent strain based multiscale modeling framework for simulating part-scale residual deformation for direct metal laser sintering. *Addit Manuf* 2019;28:406–18. DOI
  74. Bertoli US, Wolfer AJ, Matthews MJ, Delplanque JPR, Schoenung JM. On the limitations of volumetric energy density as a design parameter for selective laser melting. *Mater Des* 2017;113:331–40. DOI
  75. Prashanth KG, Scudino S, Maity T, Das J, Eckert J. Is the energy density a reliable parameter for materials synthesis by selective laser melting? *Mater Res Lett* 2017;5:386–90. DOI
  76. Greco S, Gutzeit K, Hotz H, Kirsch B, Aurich JC. Selective laser melting (SLM) of AISI 316L—impact of laser power, layer thickness, and hatch spacing on roughness, density, and microhardness at constant input energy density. *Int J Adv Manuf Techn* 2020;108:1551–62. DOI
  77. Gu H, Gong H, Pal D, et al. Influences of energy density on porosity and microstructure of selective laser melted 17-4PH stainless steel. In: 2013 Solid Freeform Fabrication Symposium. vol. 474; 2013. DOI
  78. Liu Y, Liu C, Liu W, et al. Optimization of parameters in laser powder deposition AlSi10Mg alloy using Taguchi method. *Opt Laser Techn* 2019;111:470–80. DOI
  79. King WE, Barth HD, Castillo VM, et al. Observation of keyhole-mode laser melting in laser powder-bed fusion additive manufacturing. *J Mat Proc Techn* 2014;214:2915–25. DOI
  80. Gan Z, Kafka OL, Parab N, et al. Universal scaling laws of keyhole stability and porosity in 3D printing of metals. *Nat Comm* 2021;12:1–8. DOI
  81. Rai R, Elmer J, Palmer T, DebRoy T. Heat transfer and fluid flow during keyhole mode laser welding of tantalum, Ti-6Al-4V, 304L stainless steel and vanadium. *J phys D: Appl phys* 2007;40:5753. DOI
  82. Maamoun AH, Xue YF, Elbestawi MA, Veldhuis SC. Effect of selective laser melting process parameters on the quality of al alloy parts: Powder characterization, density, surface roughness, and dimensional accuracy. *Materials* 2018;11:2343. DOI
  83. Bayat M, Thanki A, Mohanty S, et al. Keyhole-induced porosities in Laser-based Powder Bed Fusion (L-PBF) of Ti6Al4V: High-fidelity

- modelling and experimental validation. *Add Manuf* 2019;30:100835. DOI
84. Cunningham R, Zhao C, Parab N, et al. Keyhole threshold and morphology in laser melting revealed by ultrahigh-speed x-ray imaging. *Science* 2019;363:849–52. DOI
  85. Scime L, Beuth J. Melt pool geometry and morphology variability for the Inconel 718 alloy in a laser powder bed fusion additive manufacturing process. *Addit Manuf* 2019;29:100830. DOI
  86. Zhao C, Fezzaa K, Cunningham RW, et al. Real-time monitoring of laser powder bed fusion process using high-speed X-ray imaging and diffraction. *Sci rep* 2017;7:1–11. DOI
  87. Jadhav SD, Goossens LR, Kinds Y, Van Hooreweder B, Vanmeensel K. Laser-based powder bed fusion additive manufacturing of pure copper. *Addit Manuf* 2021;42:101990. DOI
  88. DebRoy T, Wei H, Zuback J, et al. Additive manufacturing of metallic components—process, structure and properties. *Progr Mat Sci* 2018;92:112–224. DOI
  89. Piglione A, Dovggy B, Liu C, et al. Printability and microstructure of the CoCrFeMnNi high-entropy alloy fabricated by laser powder bed fusion. *Materi Lett* 2018;224:22–5. DOI
  90. Sun Z, Tan X, Tor SB, Chua CK. Simultaneously enhanced strength and ductility for 3D-printed stainless steel 316L by selective laser melting. *NPG Asia Mater* 2018;10:127–36. DOI
  91. Sun Sh, Ishimoto T, Hagihara K, et al. Excellent mechanical and corrosion properties of austenitic stainless steel with a unique crystallographic lamellar microstructure via selective laser melting. *Script Mater* 2019;159:89–93. DOI
  92. Roehling TT, Shi R, Khairallah SA, et al. Controlling grain nucleation and morphology by laser beam shaping in metal additive manufacturing. *Mater Des* 2020;195:109071. DOI
  93. Kok Y, Tan XP, Wang P, et al. Anisotropy and heterogeneity of microstructure and mechanical properties in metal additive manufacturing: a critical review. *Mater Des* 2018;139:565–86. DOI
  94. Dilip J, Zhang S, Teng C, et al. Influence of processing parameters on the evolution of melt pool, porosity, and microstructures in Ti-6Al-4V alloy parts fabricated by selective laser melting. *Progr Addit Manuf* 2017;2:157–67. DOI
  95. Pham MS, Dovggy B, Hooper PA, Gourlay CM, Piglione A. The role of side-branching in microstructure development in laser powder-bed fusion. *Nat Comm* 2020;11:1–12. DOI
  96. Bustillos J, Kim J, Moridi A. Exploiting lack of fusion defects for microstructural engineering in additive manufacturing. *Addit Manuf* 2021;48:102399. DOI
  97. Körner C. Additive manufacturing of metallic components by selective electron beam melting—a review. *Int Mater Rev* 2016;61:361–77. DOI
  98. Gorsse S, Hutchinson C, Gouné M, Banerjee R. Additive manufacturing of metals: a brief review of the characteristic microstructures and properties of steels, Ti-6Al-4V and high-entropy alloys. *Sci Techn adv Mater* 2017;18:584–610. DOI
  99. Wang YM, Voisin T, McKeown JT, et al. Additively manufactured hierarchical stainless steels with high strength and ductility. *Nat Mater* 2018;17:63–71. DOI
  100. Zhang LC, Liu Y, Li S, Hao Y. Additive manufacturing of titanium alloys by electron beam melting: a review. *Adv Engin Mater* 2018;20:1700842. DOI
  101. Zhang Y, Wu L, Guo X, et al. Additive manufacturing of metallic materials: a review. *J Mater Engin Perform* 2018;27:1–13. DOI
  102. Moeinfar K, Khodabakhshi F, Kashani-bozorg S, Mohammadi M, Gerlich A. A review on metallurgical aspects of laser additive manufacturing (LAM): Stainless steels, nickel superalloys, and titanium alloys. *J Mater Res Techn* 2021;16:1029–68. DOI
  103. Guo L, Zhang L, Andersson J, Ojo O. Additive manufacturing of 18% nickel maraging steels: defect, structure and mechanical properties: A review. *J Mater Sci Techn* 2022;120:227–52. DOI
  104. Brandl E, Heckenberger U, Holzinger V, Buchbinder D. Additive manufactured AISi10Mg samples using Selective Laser Melting (SLM): Microstructure, high cycle fatigue, and fracture behavior. *Mater Des* 2012;34:159–69. DOI
  105. Spierings AB, Starr TL, Wegener K. Fatigue performance of additive manufactured metallic parts. *Rapid Prototyping J* 2013. DOI
  106. Ion JC, Shercliff HR, Ashby MF. Diagrams for laser materials processing. *Acta Metall Et Mater* 1992;40:1539–51. DOI
  107. Beuth J, Klingbeil N. The role of process variables in laser-based direct metal solid freeform fabrication. *JoM* 2001;53:36–9. DOI
  108. Beuth J, Fox J, Gockel J, et al. Process mapping for qualification across multiple direct metal additive manufacturing processes. In: *Solid freeform fabrication proceedings*. Univ. Tex. Austin; 2013. pp. 655–65. DOI
  109. Tran HC, Lo YL. Systematic approach for determining optimal processing parameters to produce parts with high density in selective laser melting process. *Int J Adv Manuf Techn* 2019;105:4443–60. DOI
  110. Johnson L, Mahmoudi M, Zhang B, et al. Assessing printability maps in additive manufacturing of metal alloys. *Act Mater* 2019;176:199–210. DOI
  111. Thomas M, Baxter GJ, Todd I. Normalised model-based processing diagrams for additive layer manufacture of engineering alloys. *Acta Mater* 2016;108:26–35. DOI
  112. Rubenchik AM, King WE, Wu SS. Scaling laws for the additive manufacturing. *J Mater Proc Techn* 2018;257:234–43. DOI
  113. Hann D, Iammi J, Folkes J. A simple methodology for predicting laser-weld properties from material and laser parameters. *J Phys D: Appl Phys* 2011;44:445401. DOI
  114. Wang Z, Liu M. Dimensionless analysis on selective laser melting to predict porosity and track morphology. *J Mater Proc Techn* 2019;273:116238. DOI
  115. Mukherjee T, Manvatkar V, De A, DebRoy T. Dimensionless numbers in additive manufacturing. *J Appl Phys* 2017;121:064904. DOI
  116. Van Elsen M, Al-Bender F, Kruth JP. Application of dimensional analysis to selective laser melting. *Rapid Prot J* 2008;14:15–22. DOI

117. Mukherjee T, Zuback J, De A, DebRoy T. Printability of alloys for additive manufacturing. *Sci rep* 2016;6:1–8. DOI
118. Tang M, Pistorius PC, Beuth JL. Prediction of lack-of-fusion porosity for powder bed fusion. *Addit Manuf* 2017;14:39–48. DOI
119. Gordon JV, Narra SP, Cunningham RW, et al. Defect structure process maps for laser powder bed fusion additive manufacturing. *Addit Manuf* 2020;36:101552. DOI
120. Zhang B, Seede R, Xue L, et al. An efficient framework for printability assessment in laser powder bed fusion metal additive manufacturing. *Addit Manuf* 2021:102018. DOI
121. Spierings AB, Levy G. Comparison of density of stainless steel 316L parts produced with selective laser melting using different powder grades. In: Proceedings of the Annual International Solid Freeform Fabrication Symposium. Austin, TX; 2009. pp. 342–53. DOI
122. Bidare P, Maier RRJ, Beck RJ, Shephard JD, Moore AJ. An open-architecture metal powder bed fusion system for in-situ process measurements. *Addit Manuf* 2017;16:177–85. DOI
123. Jansen D, Hanemann T, Radek M, et al. Development of actual powder layer height depending on nominal layer thicknesses and selection of laser parameters. *J Mater Proc Techn* 2021;298:117305. DOI
124. Ahn IH. Determination of a process window with consideration of effective layer thickness in SLM process. *Int J Adv Manuf Techn* 2019;105:4181–91. DOI
125. Gockel J, Sheridan L, Koerper B, Whip B. The influence of additive manufacturing processing parameters on surface roughness and fatigue life. *Int J Fat* 2019;124:380–8. DOI
126. Qian C, Xu H, Zhong Q. The influence of process parameters on corrosion behavior of Ti6Al4V alloy processed by selective laser melting. *J Laser Appl* 2020;32:032010. DOI
127. Vukkum V, Gupta R. Review on corrosion performance of laser powder-bed fusion printed 316L stainless steel: effect of processing parameters, Manufacturing defects, post-processing, feedstock, and microstructure. *Mater Des* 2022:110874. DOI
128. McGregor M, Patel S, McLachlin S, Vlasea M. Architectural bone parameters and the relationship to titanium lattice design for powder bed fusion additive manufacturing. *Addit Manuf* 2021;47:102273. DOI
129. Blakey-Milner B, Gradl P, Snedden, et al. Metal additive manufacturing in aerospace: a review. *Mater Des* 2021;209:110008. DOI
130. Vasco JC. Additive manufacturing for the automotive industry. In: *Addit Manuf*. Elsevier; 2021. pp. 505–30. DOI
131. Elsayed M, Ghazy M, Youssef Y, Essa K. Optimization of SLM process parameters for Ti6Al4V medical implants. *Rapid Prot J* 2019;25:433–47. DOI
132. Yang Y, Lu Jb, Luo ZY, Wang D. Accuracy and density optimization in directly fabricating customized orthodontic production by selective laser melting. *Rap Prot J* 2012;18:482–9. DOI
133. Rej R. NIST/SEMATECH e-handbook of statistical methods; 2003. DOI
134. Sun J, Yang Y, Wang D. Parametric optimization of selective laser melting for forming Ti6Al4V samples by Taguchi method. *Opt Laser Techn* 2013;49:118–24. DOI
135. Yakout M, Elbestawi M, Veldhuis SC. Density and mechanical properties in selective laser melting of Invar 36 and stainless steel 316L. *J Mater Proc Techn* 2019;266:397–420. DOI
136. Wang D, Liu Y, Yang Y, Xiao D. Theoretical and experimental study on surface roughness of 316L stainless steel metal parts obtained through selective laser melting. *Rap Prot J* 2016;22:706–16. DOI
137. Wang C, Tan X, Liu E, Tor SB. Process parameter optimization and mechanical properties for additively manufactured stainless steel 316L parts by selective electron beam melting. *Mater Des* 2018;147:157–66. DOI
138. Gong H, Gu H, Zeng K, et al. Melt pool characterization for selective laser melting of Ti-6Al-4V pre-alloyed powder. In: Solid freeform fabrication symposium; 2014. pp. 256–67. DOI
139. Mutua J, Nakata S, Onda T, Chen ZC. Optimization of selective laser melting parameters and influence of post heat treatment on microstructure and mechanical properties of maraging steel. *Mater Des* 2018;139:486–97. DOI
140. Gong H, Rafi K, Gu H, Starr T, Stucker B. Analysis of defect generation in Ti-6Al-4V parts made using powder bed fusion additive manufacturing processes. *Addit Manuf* 2014;1:87–98. DOI
141. Bhardwaj T, Shukla M, Paul C, Bindra K. Direct energy deposition-laser additive manufacturing of titanium-molybdenum alloy: Parametric studies, microstructure and mechanical properties. *J Alloys Comp* 2019;787:1238–48. DOI
142. Diaz Vallejo N, Lucas C, Ayers N, et al. Process optimization and microstructure analysis to understand laser powder bed fusion of 316L stainless steel. *Metals* 2021;11:832. DOI
143. Dong D, Chang C, Wang H, et al. Selective laser melting (SLM) of CX stainless steel: theoretical calculation, process optimization and strengthening mechanism. *J Mater Sci Techn* 2021;73:151–64. DOI
144. Oyesola M, Mpofu K, Mathe N, et al. Optimization of selective laser melting process parameters for surface quality performance of the fabricated Ti6Al4V. *Int J Adv Manuf Techn* 2021;114:1585–99. DOI
145. Shrestha S, Manogharan G. Optimization of binder jetting using Taguchi method. *JOM* 2017;69:491–7. DOI
146. Chen H, Zhao YF. Process parameters optimization for improving surface quality and manufacturing accuracy of binder jetting additive manufacturing process. *Rap Prot J* 2016;22:527–38. DOI
147. Sobester A, Forrester A, Keane A. Engineering design via surrogate modelling: a practical guide. John Wiley & Sons; 2008. DOI
148. Thomas DS, Gilbert SW. Costs and cost effectiveness of additive manufacturing. *NIST Spec Public* 2014;1176:12. DOI
149. Dada M, Popoola P, Aramide O, Mathe N, Pityana S. Optimization of the corrosion property of a high entropy alloy using response surface methodology. *Mater Today: Proc* 2021;38:1024–30. DOI
150. Dowling L, Kennedy J, O’shaughnessy S, Trimble D. A review of critical repeatability and reproducibility issues in powder bed fusion. *Mat Des* 2020;186:108346. DOI

151. Aboutaleb AM, Bian L, Elwany A, et al. Accelerated process optimization for laser-based additive manufacturing by leveraging similar prior studies. *IJSE Trans* 2017;49:31–44. DOI
152. Plotkowski A, Kirka MM, Babu S. Verification and validation of a rapid heat transfer calculation methodology for transient melt pool solidification conditions in powder bed metal additive manufacturing. *Addit Manuf* 2017;18:256–68. DOI
153. Wang L, Zhang Y, Yan W. Evaporation model for keyhole dynamics during additive manufacturing of metal. *Phys Rev Appl* 2020;14:064039. DOI
154. Yang M, Wang L, Yan W. Phase-field modeling of grain evolutions in additive manufacturing from nucleation, growth, to coarsening. *Npj Comput Mater* 2021;7:1–12. DOI
155. Grilli N, Hu D, Yushu D, Chen F, Yan W. Crystal plasticity model of residual stress in additive manufacturing using the element elimination and reactivation method. *Comput Mech* 2021;1–21. DOI
156. Yadollahi A, Shamsaei N. Additive manufacturing of fatigue resistant materials: challenges and opportunities. *Int J Fat* 2017;98:14–31. DOI
157. Yang Y, Allen M, London T, Oancea V. Residual strain predictions for a powder bed fusion Inconel 625 single cantilever part. *Int Mater Manuf Innov* 2019;8:294–304. DOI
158. Li C, Liu J, Fang X, Guo Y. Efficient predictive model of part distortion and residual stress in selective laser melting. *Addit Manuf* 2017;17:157–68. DOI
159. Qu M, Guo Q, Escano LI, et al. Controlling process instability for defect lean metal additive manufacturing. *Nat Comm* 2022;13:1–8. DOI
160. Markl M, Körner C. Multiscale modeling of powder bed-based additive manufacturing. *Ann Rev Mater Res* 2016;46:93–123. DOI
161. Wei H, Mukherjee T, Zhang W, et al. Mechanistic models for additive manufacturing of metallic components. *Progr Mater Sci* 2021;116:100703. DOI
162. Kouraytem N, Li X, Tan W, Kappes B, Spear AD. Modeling process–structure–property relationships in metal additive manufacturing: a review on physics-driven versus data-driven approaches. *J Phys: Mater* 2021;4:032002. DOI
163. Promoppatum P, Yao SC, Pistorius PC, Rollett AD. A comprehensive comparison of the analytical and numerical prediction of the thermal history and solidification microstructure of Inconel 718 products made by laser powder-bed fusion. *Engineering* 2017;3:685–94. DOI
164. Yang X, Barrett RA, Harrison NM, Leen SB. A physically-based structure-property model for additively manufactured Ti-6Al-4V. *Mater Des* 2021;205:109709. DOI
165. Khairallah SA, Anderson AT, Rubenchik A, King WE. Laser powder-bed fusion additive manufacturing: physics of complex melt flow and formation mechanisms of pores, spatter, and denudation zones. *Act Mater* 2016;108:36–45. DOI
166. Yan W, Qian Y, Ge W, Lin S, Liu WK, et al. Meso-scale modeling of multiple-layer fabrication process in selective electron beam melting: inter-layer/track voids formation. *Mater Des* 2018;141:210–9. DOI
167. Jiang P, Zhou Q, Shao X. Surrogate model-based engineering design and optimization. Springer; 2020. DOI
168. Tapia G, Khairallah S, Matthews M, King WE, Elwany A. Gaussian process-based surrogate modeling framework for process planning in laser powder-bed fusion additive manufacturing of 316L stainless steel. *Int J Adv Manuf Techn* 2018;94:3591–603. DOI
169. Aoyagi K, Wang H, Sudo H, Chiba A. Simple method to construct process maps for additive manufacturing using a support vector machine. *Addit manuf* 2019;27:353–62. DOI
170. Wang C, Tan X, Tor S, Lim C. Machine learning in additive manufacturing: State-of-the-art and perspectives. *Addit Manuf* 2020;36:101538. DOI
171. DebRoy T, Mukherjee T, Wei H, Elmer J, Milewski J. Metallurgy, mechanistic models and machine learning in metal printing. *Nat Revi Mat* 2020;1–21. DOI
172. Meng L, McWilliams B, Jarosinski W, et al. Machine learning in additive manufacturing: a review. *JoM* 2020;72:2363–77. DOI
173. Yeung H, Yang Z, Yan L. A melt pool prediction based scan strategy for powder bed fusion additive manufacturing. *Addit Manuf* 2020;35:101383. DOI
174. Wang Z, Liu P, Xiao Y, et al. A data-driven approach for process optimization of metallic additive manufacturing under uncertainty. *J Manuf Sci Engin* 2019;141. DOI
175. Mondal S, Gwynn D, Ray A, Basak A. Investigation of melt pool geometry control in additive manufacturing using hybrid modeling. *Metals* 2020;10:683. DOI
176. Narayana PL, Kim JH, Lee J, et al. Optimization of process parameters for direct energy deposited Ti-6Al-4V alloy using neural networks. *Int J Adv Manuf Techn* 2021:1–15. DOI
177. Nguyen DS, Park HS, Lee CM. Optimization of selective laser melting process parameters for Ti-6Al-4V alloy manufacturing using deep learning. *J Manuf Proc* 2020;55:230–5. DOI
178. Kappes B, Moorthy S, Drake D, Geerlings H, Stebner A. Machine learning to optimize additive manufacturing parameters for laser powder bed fusion of Inconel 718. In: Proceedings of the 9th international symposium on superalloy 718 & derivatives: Energy, aerospace, and industrial applications. Springer; 2018. pp. 595–610. DOI
179. Tapia G, Elwany AH, Sang H. Prediction of porosity in metal-based additive manufacturing using spatial Gaussian process models. *Addit Manuf* 2016;12:282–90. DOI
180. Kamath C. Data mining and statistical inference in selective laser melting. *Int J Adv Manuf Techn* 2016;86:1659–77. DOI
181. Meng L, Zhang J. Process design of laser powder bed fusion of stainless steel using a Gaussian process-based machine learning model. *JoM* 2020;72:420–8. DOI

182. Williams CK, Rasmussen CE. Gaussian processes for machine learning, vol. 2. MIT press Cambridge, MA; 2006. DOI
183. Goel T, Haftka RT, Shyy W, Queipo NV. Ensemble of surrogates. *Struct Multidisc Optim* 2007;33:199–216. DOI
184. Wang GG, Shan S. Review of metamodeling techniques in support of engineering design optimization. *J Mech Des Apr* 2007;129:370–80. DOI
185. An D, Kim NH, Choi JH. Practical options for selecting data-driven or physics-based prognostics algorithms with reviews. *Reli Engin Syst Saf* 2015;133:223–36. DOI
186. Younis A, Dong Z. Trends, features, and tests of common and recently introduced global optimization methods. *Engin Optimiz* 2010;42:691–718. DOI
187. Dong H, Li C, Song B, Wang P. Multi-surrogate-based differential evolution with multi-start exploration (MDEME) for computationally expensive optimization. *Adv Engin Softw* 2018;123:62–76. DOI
188. Diaz-Manriquez A, Toscano G, Coello Coello CA. Comparison of metamodeling techniques in evolutionary algorithms. *Soft Comp* 2017;21:5647–63. DOI
189. Jin R, Chen W, Simpson TW. Comparative studies of metamodeling techniques under multiple modelling criteria. *Struct Mult Optim* 2001;23:1–13. DOI
190. Yadroitsev I, Krakhmalev P, Yadroitsava I, Johansson S, Smurov I. Energy input effect on morphology and microstructure of selective laser melting single track from metallic powder. *J Mater Proc Techn* 2013;213:606–13. DOI
191. Liu J, Song Y, Chen C, et al. Effect of scanning speed on the microstructure and mechanical behavior of 316L stainless steel fabricated by selective laser melting. *Mater Des* 2020;186:108355. DOI
192. Leicht A, Fischer M, Klement U, Nyborg L, Hryha E. Increasing the productivity of laser powder bed fusion for stainless steel 316L through increased layer thickness. *J Mater Engin Perf* 2021;30:575–84. DOI
193. Wu J, Zhang S, Sun J, Zhang C. Data-driven multi-objective optimization of laser welding parameters of 6061-T6 aluminum alloy. *J Phys: Conf Ser* 2021 apr;1885:042007. DOI
194. Zhang P, Zhang C, Liu L. Toughening 3D-printed Zr-based bulk metallic glass via synergistic defects engineering. *Mater Res Lett* 2022;10:377–84. DOI
195. Coello CAC, Lamont GB, Van Veldhuizen DA, et al. Evolutionary algorithms for solving multi-objective problems. vol. 5. Springer; 2007. DOI
196. Rao SS. Engineering optimization: theory and practice. John Wiley & Sons; 2019. DOI
197. Aboutaleb AM, Mahtabi MJ, Tschopp MA, Bian L. Multi-objective accelerated process optimization of mechanical properties in laser-based additive manufacturing: Case study on Selective Laser Melting (SLM) Ti-6Al-4V. *J Manuf Proc* 2019;38:432–44. DOI
198. Padhye N, Deb K. Multi-objective optimisation and multi-criteria decision making in SLS using evolutionary approaches. *Rapid Prot J* 2011. DOI
199. Yan J, Battiato I, Fadel GM. A mathematical model-based optimization method for Direct Metal Deposition of multimaterials. *J Manuf Sci Engin* 2017;139. DOI
200. Strano G, Hao L, Everson R, Evans K. Multi-objective optimization of selective laser sintering processes for surface quality and energy saving. *Proc Inst Mech Engin, Part B: J Engin Manuf* 2011;225:1673–82. DOI
201. Meng L, Zhao J, Lan X, Yang H, Wang Z. Multi-objective optimisation of bio-inspired lightweight sandwich structures based on selective laser melting. *Virt Phys Prot* 2020;15:106–19. DOI
202. Li J, Hu J, Cao L, et al. Multi-objective process parameters optimization of SLM using the ensemble of metamodels. *J Manuf Proc* 2021;68:198–209. DOI
203. Deb K, Pratap A, Agarwal S, Meyarivan T. A fast and elitist multiobjective genetic algorithm: NSGA-II. *IEEE trans evolcomput* 2002;6:182–97. DOI
204. Asadollahi-Yazdi E, Gardan J, Lafon P. Multi-objective optimization approach in design for additive manufacturing for fused deposition modeling. *Rapid Prot J* 2019;25:875–87. DOI
205. Wu J, Lian K, Deng Y, Jiang P, Zhang C. Multi-objective parameter optimization of fiber laser welding considering energy consumption and bead geometry. *IEEE Trans Autom Sci Engin* 2021:1–14. DOI
206. Jiang P, Cao L, Zhou Q, et al. Optimization of welding process parameters by combining Kriging surrogate with particle swarm optimization algorithm. *Int J Adv Manuf Techn* 2016;86:2473–83. DOI
207. Padhye N. Topology optimization of compliant mechanism using multi-objective particle swarm optimization. In: Proceedings of the 10th annual conference companion on genetic and evolutionary computation; 2008. pp. 1831–4. DOI
208. Zhang Y, Wang S, Ji G. A comprehensive survey on particle swarm optimization algorithm and its applications. *Math Probl Engin* 2015;2015. DOI
209. Aboutaleb AM, Tschopp MA, Rao PK, Bian L. Multi-objective accelerated process optimization of part geometric accuracy in additive manufacturing. *J Manuf Sci Engin* 2017;139. DOI
210. Mukherjee T, DebRoy T. Printability of 316 stainless steel. *Sci Techn Weld Join* 2019;24:412–9. DOI
211. Campagnoli MR, Galati M, Saboori A. On the processability of copper components via powder-based additive manufacturing processes: Potentials, challenges and feasible solutions. *J Manuf Proc* 2021;72:320–37. DOI
212. Xie X, Bennett J, Saha S, et al. Mechanistic data-driven prediction of as-built mechanical properties in metal additive manufacturing. *npj Comput Mater* 2021;7:1–12. DOI
213. Du Y, Mukherjee T, DebRoy T. Physics-informed machine learning and mechanistic modeling of additive manufacturing to reduce defects. *Appl Mater Today* 2021;24:101123. DOI

214. Loh GH, Pei E, Harrison D, Monzón MD. An overview of functionally graded additive manufacturing. *Add Manuf* 2018;23:34–44. DOI
215. Shi R, Khairallah SA, Roehling TT, et al. Microstructural control in metal laser powder bed fusion additive manufacturing using laser beam shaping strategy. *Acta Mater* 2020;184:284–305. DOI
216. Tey CF, Tan X, Sing SL, Yeong WY. Additive manufacturing of multiple materials by selective laser melting: Ti-alloy to stainless steel via a Cu-alloy interlayer. *Addit Manuf* 2020;31:100970. DOI
217. Anstaett C, Seidel C, Reinhart G. Fabrication of 3D multi-material parts using laser-based powder bed fusion. In: Proceedings of the 28th Annual International Solid Freeform Fabrication Symposium; 2017. Available from: <https://hdl.handle.net/2152/89963> [Last accessed on 22 Sep].